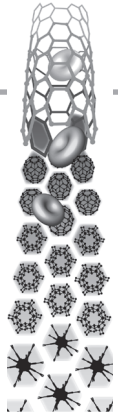

Molecular plasmonics for biology and nanomedicine

The optical excitation of surface plasmons in metal nanoparticles leads to nanoscale spatial confinement of electromagnetic fields. The confined electromagnetic fields can generate intense, localized thermal energy and large near-field optical forces. The interaction between these effects and nearby molecules has led to the emerging field known as molecular plasmonics. Recent advances in molecular plasmonics have enabled novel optical materials and devices with applications in biology and nanomedicine. In this article, we categorize three main types of interactions between molecules and surface plasmons: optical, thermal and mechanical. Within the scope of each type of interaction, we will review applications of molecular plasmonics in biology and nanomedicine. We include a wide range of applications that involve sensing, spectral analysis, imaging, delivery, manipulation and heating of molecules, biomolecules or cells using plasmonic effects. We also briefly describe the physical principles of molecular plasmonics and progress in the nanofabrication, surface functionalization and bioconjugation of metal nanoparticles.

KEYWORDS: drug delivery ▪ gene switches ▪ localized surface plasmon resonance ▪ molecular plasmonics ▪ nanocarrier ▪ nanosensor ▪ photothermal therapeutics ▪ plasmonic nanoscopy ▪ plasmonic tweezers ▪ surface-enhanced Raman spectroscopy

Yue Bing Zheng[1,2,3], Brian Kiraly[4], Paul S Weiss*[1,2,3] & Tony Jun Huang*[4]

[1]*California NanoSystems Institute, University of California, Los Angeles, CA 90095, USA*
[2]*Department of Chemistry & Biochemistry, University of California, Los Angeles, Los Angeles, CA 90095, USA*
[3]*Department of Materials Science & Engineering, University of California, Los Angeles, Los Angeles, CA 90095, USA*
[4]*Department of Engineering Science & Mechanics, The Pennsylvania State University, University Park, PA 16802, USA*
**Authors for correspondence:*
Tel.: +1 814 863 4209
Fax: +1 814 865 9974
junhuang@psu.edu
Tel.: +1 310 267 5993
Fax: +1 310 267 4918
psw@cnsi.ucla.edu

Localized surface plasmon resonance (LSPR) occurs in metal nanoparticles when light drives the oscillation of the free electrons in the nanoparticle [1]. A schematic illustration of LSPR is shown in Figure 1A: when external light is incident on a metal nanoparticle, its electric field (E_0) periodically displaces the sphere's electrons with respect to the lattice ions, resulting in oscillating electron density [2]. Upon the excitation of LSPR, nanoscale localization and enhancement of electromagnetic (EM) fields occur in the vicinity of the metal nanoparticle [3]. The locally enhanced EM fields generate localized thermal energy because of the rapid conversion of photon energy into heat via electron–electron scattering and electron–phonon coupling [4] and strongly scatter and absorb light at the LSPR wavelengths (Figure 1B) [5–12].

These nanoscale fields can interact with cells, large biomolecules and even small molecules, optically, thermally and mechanically. By understanding and controlling the interactions between these objects and surface plasmons, researchers have developed approaches for efficiently sensing, analyzing, trapping, transporting and manipulating molecules and cells [13–20]. These developments have led to novel devices and analytical tools for applications in biology and nanomedicine and to the formation of the field of molecular plasmonics (Figure 2). For example, because the highly concentrated light near the particles is sensitive to molecular dynamics, the metal nanoparticles can function as sensors for understanding molecular-level biological processes [21–25]. With the increased scattering and/or absorption cross sections, metal nanoparticles are extremely sensitive labels for immunoassays and molecular spectroscopy [26]. In addition, researchers have successfully demonstrated plasmonic photothermal therapy for cancer based on the strong localization of photothermal energy [27–33]. The high intensity and large gradient of EM fields associated with LSPR in the particles' near field result in powerful optical forces that are the foundation for plasmonic tweezers used for single-molecule biophysics [34,35]. Implementing the valuable properties of molecular plasmonics in practical applications, however, is subject to the development of both plasmonics and molecular nanotechnology.

Due to the small size of single molecules, molecular plasmonics requires precise control of both the spatial profile of surface plasmons and the location of molecules within the near field of metal nanoparticles, in order to have effective molecule–plasmon interactions. *In vivo* applications have additional requirements on the shape, size, LSPR wavelength and surface functionalization of the metal nanoparticles for targeted delivery, imaging and plasmonic excitation inside human bodies [36,37]. Recent progress in nanofabrication, measurement methods,

Future Medicine part of fsg

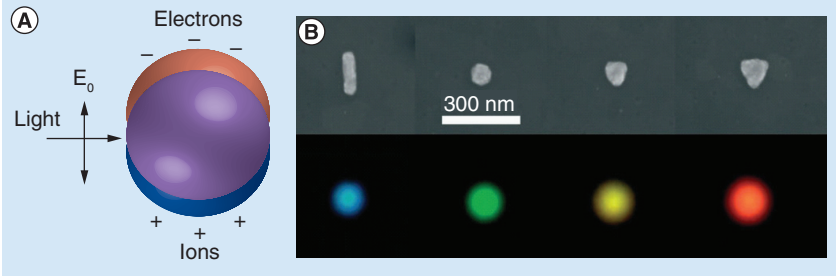

Figure 1. Basic principles of localized surface plasmon resonance. **(A)** Schematic shows that, when an external light wave is incident on a silver nanosphere, its electric field, E_0, periodically displaces the sphere's electrons with respect to the lattice. This results in oscillating electron density – a localized surface plasmon resonance. **(B)** Scanning electron micrographs (top) and dark-field images (bottom) of several metal nanoparticles made by electron beam lithography. From left to right the shapes are a rod, a disc and two triangles.
Reproduced with permission from [5] © WILEY-VCH Verlag GmbH & Co. KGaA, Weinheim (2007).

instruments, metrology and computation enable the precise modeling, design and control of both near- and far-field LSPR profiles at a wide range of wavelengths (Figure 3) [38–46]. These developments have granted vital temporal, spatial and spectral control of the plasmon–molecule interactions.

Both 'bottom-up' chemical synthesis and 'top-down' lithographic techniques have been highly developed for the fabrication of metal nanoparticles [41,47–49]. While the former provides crystalline nanoparticles allowing extremely precise control of their shape, size and composition by assembling the particles atom-by-atom, the latter allows flexibility in controlling particle shape and size in arbitrary 2D arrays fixed on substrates. Figure 4 shows examples of 2D metal nanostructure arrays fabricated with nanosphere lithography [43] or electron beam lithography [50]. In these arrays, coupling between nanoparticles provides another degree of freedom for controlling the spectral and spatial properties of surface plasmons [51]. A dramatic enhancement of the localized EM fields is achievable by gaining materials at the metal nanostructures, as demonstrated in the development of surface plasmon amplification by stimulated emission of radiation [52,53].

Along with developments in the fabrication of metal nanoparticles, good progress has been made in molecular functionalization, self-assembly and measurement tools that enable precise position and characterization of molecules and biomolecules on metal surfaces (Figure 5) [54–62]. These advances in both plasmonics and molecular nanotechnology have gradually shifted the focus of molecular plasmonics from developing high-quality metal nanostructure–molecule complexes and investigating their physical properties to the potential applications of these complexes.

In this article, we aim to review the recent developments in molecular plasmonics, which include a broad range of biological/medical applications. We categorize and discuss representative applications of molecular plasmonics within the framework of three types of molecule–plasmon interactions: optical, thermal and mechanical. These applications include sensing, spectroscopy, imaging, phototherapy, nanocarriers and plasmonic tweezers. Finally, we present the current challenges and future research directions for each application.

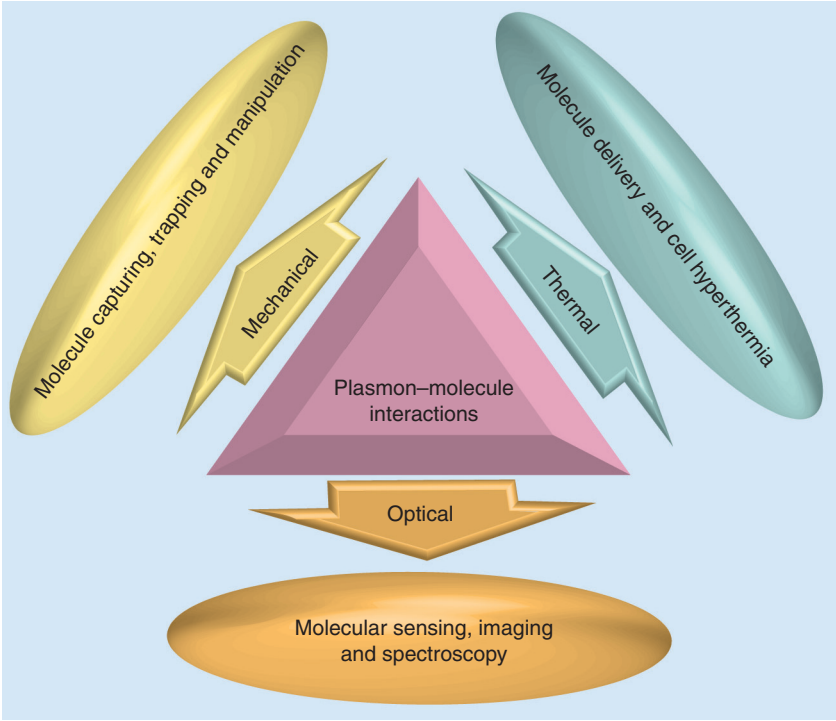

Figure 2. Schematic summarizing and structuring biological and nanomedical applications of molecular plasmonics. Three types of molecule–plasmon interactions – optical, mechanical and thermal – underpin emerging applications in molecular biology and nanomedicine.

Applications based on optical effects

Nanosensors based on LSPR modulation

Molecular detection with high sensitivity is an invaluable assay for elucidating biomolecular interactions and dynamics at the smallest scales [21]. Plasmon resonance is exquisitely sensitive to changes in the refractive index surrounding the nanoparticles because of the nanoscale localization and enhancement of the EM field [24,63]. By monitoring the intense, narrow LSPR spectra in either the extinction or scattering modes, we can detect molecule-induced changes in the local refractive index through LSPR modulations [64].

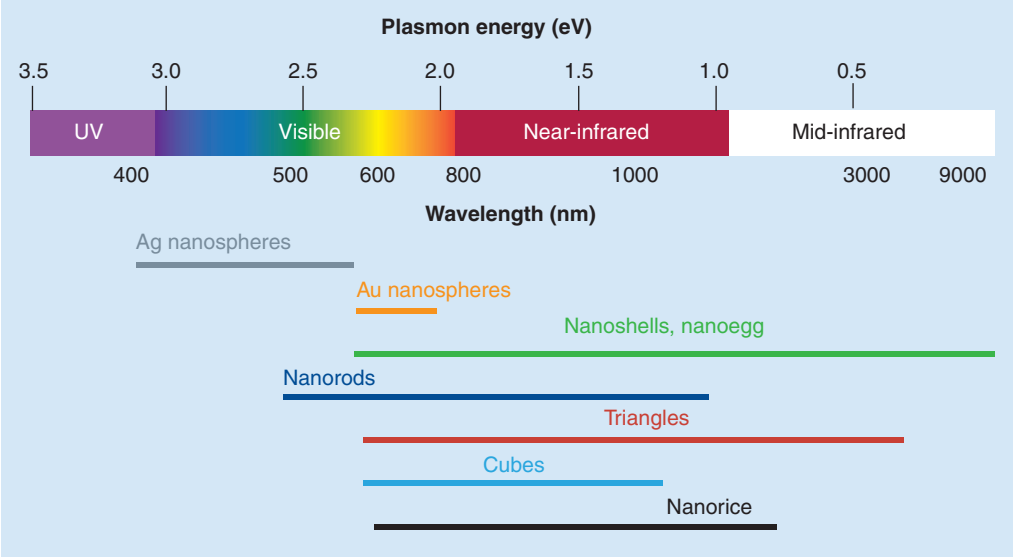

Figure 3. Localized surface plasmon resonance range of metal nanoparticles of different shapes. A wide range (from UV to mid-infrared) of localized surface plasmon resonance wavelengths are obtained with metal nanoparticles of various shapes and sizes.
Reproduced with permission from [39] © 2007 Nature Publishing Group.

Specifically, the LSPR peak wavelength, intensity and/or bandwidth can be modulated by molecular adsorption, desorption or even conformational changes that induce variations in the refractive index [65–68]. Furthermore, the size of the nanoparticles endows them with excellent spatial resolution that is of considerable value when delivered inside the human body for *in vivo* applications [69].

With simple, inexpensive transmission spectrometry, LSPR-modulation-based sensors have been making tremendous progress in detecting molecules, biomolecules and cellular signaling [19,21,25,64,70–72]. Yonzon and coworkers studied the real-time binding of conconavalin A to mannose-functionalized nanoparticles [73]. Haes *et al.* used LSPR nanosensors to measure amyloid-derived diffusible ligands at a concentrations of 100 fM [71]. Alivisatos and coworkers developed a plasmonic molecular ruler, which monitors LSPR modulation from changes in plasmonic coupling between a pair of metal nanoparticles, to detect the hybridization of DNA oligonucleotides to ssDNA [74,75]. Recently, 3D plasmonic molecular rulers have been developed based on coupled plasmonic oligomers; the 3D rulers enable retrieval of the complete spatial configuration of biological processes and their dynamic evolution [76]. Atwater and coworkers developed compliant plasmonic metamaterials [77]. By integrating split-ring resonators on polydimethylsiloxane, mechanical deformation was used to change the capacitance of the gap and the coupling strength between the resonators, thus tuning and customizing the response of the metamaterials postfabrication. Compliant metamaterials could both detect small changes in refractive index and resonantly enhance the vibrational modes of molecules [77].

A significant milestone for LSPR nanosensors is to reach the single-molecule detection limit [13]. This can be achieved by improving the sensitivity of the metal nanoparticles with new structures [78–83], improving the resolution of spectrometers [84] and/or increasing the effective change in the dielectric constant per molecular binding event [85,86]. The final option requires a better understanding of plasmon–molecule interactions, and in that vein, by exploiting the electronic couplings between molecular resonances and nanoparticle LSPR, researchers have uncovered three scenarios that exhibit surprisingly large changes in the LSPR. Figure 6 shows three scenarios for the evolution of the LSPR spectra upon adsorption of resonant molecules. The molecular resonances lead to strong absorption by the molecules at their resonant wavelengths, usually known as exciton absorption. We provide a detailed discussion on each scenario below.

As illustrated in scenario 1 in Figure 6, a large LSPR shift arises from the adsorption of resonant molecules onto metal nanoparticles. The large LSPR shift arises due to the spectral overlap between the LSPR and the molecular absorbance, which causes a significant change in the local refractive index as described by the

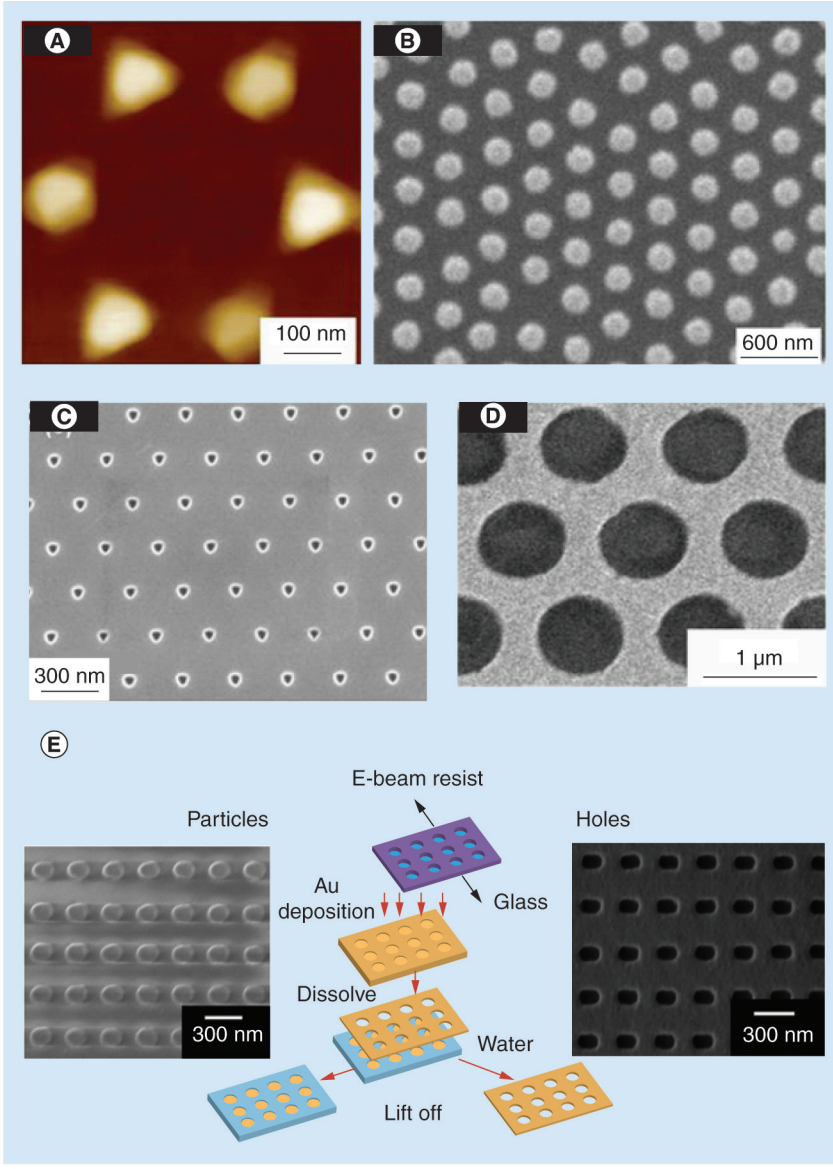

Figure 4. Examples of metal nanoparticle arrays produced using various nanofabrication techniques. (A–D) Nanoprisms, nanodisks, triangular nanoholes and circular nanoholes, respectively, made with nanosphere lithography. **(E)** The fabrication of nanoparticle and complementary nanohole structures with electron beam lithography, with scanning electron microscopy images of nanoparticle and nanohole arrays.
(A–D) Reproduced with permission from [43] © Elsevier (2008). **(E)** Reproduced with permission from [50] © 2010 American Institute of Physics.

Kramer–Kronig relations (see the 'experimental' column of scenario 1 in Figure 6) [87]. In Figure 7A, a monolayer of [2,3,7,8,12,13,17,18-octakis-(propyl)porphyrazinato]magnesium (II) with molecular resonance at 598 nm adsorbed on the silver nanoparticles of different LSPRs is shown [87]. When the LSPR wavelength is much larger or smaller than 598 nm, a redshift of approximately 20 nm is observed upon molecular adsorption. When the LSPR wavelength is equal to 598 nm, an unusually small redshift of only 2 nm is observed. However, when the LSPR is redshifted 6 nm from 598 nm (i.e., at 604 nm) an unusually large redshift of approximately 60 nm occurs. This exquisite sensitivity to molecular absorption paves the way for the development of highly tuned sensors based on shifts in molecular absorbance in response to analyte concentrations. These sensors transduce weak changes in molecular absorption intensity or wavelength into spectral shifts in the intense LSPR scattering and absorbance signals (Figure 7B) [85]. In the second scenario (scenario 2 in Figure 6), the electronic coupling between the LSPR and molecular resonance leads to plasmon resonance energy transfer and wavelength-specific quenching shown as a dip in the Rayleigh scattering spectrum of the nanoparticle–molecule complexes [88]. Monitoring this quenching leads to development of a new type of molecule-level sensors [86]. Based on plasmon resonance energy transfer spectroscopy, real-time production of cytochrome c in living HepG2 cells has been imaged [89]. In scenario 3, as illustrated in the schematic column of Figure 6, the LSPR and molecular resonances hybridize and two new resonances appear on either side (one redshifted and one blueshifted) of the original LSPR. Wiederrecht *et al.* reported the hybridization in J-aggregate–metal nanosphere complexes [90]. Halas and coworkers studied wavelength-dependent coupling behavior in hybrid nanostructures composed of Au nanoshells and J-aggregates [91]. The Au nanoshells enabled facile tuning of the LSPR wavelength over a wide spectral range surrounding the absorption peak of the J-aggregate. Both asymmetric energy splitting and anti-crossing behavior were observed in the coupled energy diagram (see the experimental column of scenario 3 of Figure 6). Wang and coworkers used colloidal Au nanorods to study resonance coupling both collectively and individually [92–94]. To overcome challenges involving the fixed nature of LSPR in metal nanoparticles, Zheng *et al.* developed tunable plasmonic systems that enable the incident angle of light to modify the LSPR spectrum (Figure 8) [95]. The tunable systems allow researchers to explore and understand coupling in both weak and strong regimes with a single nanoparticle structure [65,95]. In the near future, we expect to see cases that utilize the hybridization phenomena for sensing applications.

In summary, the EM fields associated with LSPR near metal nanoparticles are extremely sensitive to their surroundings. This high sensitivity, in combination with the advantages of light (e.g., noninvasiveness, high speed and

directionality), makes plasmonic nanosensors attractive for studying biological molecules and reactions. A broad range of applications have already been demonstrated. Continuous improvements in sensitivity and selectivity are being achieved through progress in multiple aspects: design, modeling and fabrication of metal nanostructures; surface functionalization and bioconjugation; and understanding plasmon–molecule resonant interactions. Many researchers are currently working to push these devices toward single-molecule sensitivity. One of the major (seemingly insurmountable) challenges for LSPR-modulation-based nanosensors is to identify unknown molecules. Currently, we apply other techniques, such as MALDI mass spectrometry [96] and surface-enhanced Raman spectroscopy (SERS) [3], to circumvent these problems.

SERS

Raman spectroscopy is a highly specific technique used to detect and to identify molecules based on their unique vibrational energy levels and corresponding Raman fingerprints [97]. In Raman scattering, photons are scattered inelastically, either losing energy (Stokes shift) or gaining energy (anti-Stokes shift) equal to the molecular vibrations of the probed material. One challenge for conventional Raman spectroscopy is detecting small amounts of molecules: the low Raman scattering efficiency of single molecules generally results in weak Raman signals for low concentrations. Plasmon-enhanced EM fields, however, are capable of amplifying Raman signals from molecules near the particles, leading to highly sensitive molecular identification (FIGURE 9) [18,98,99]. Advances in plasmonics have enabled the generation and control of EM hot spots with extremely high intensity and helped understand the effects of the spectral overlap between the excitation laser and LSPR on the Raman enhancement factor, leading to rational design of plasmonic nanostructures for maximum enhancement of Raman signals [64,100]. Recently, Le Ru and coworkers proposed a simple scheme and a general experimental methodology based on selective adsorption of the target analyte only at the SERS hotspots that enables detection of every single target molecule in solution [101]. Liz-Marzan and Alvarez-Puebla developed a universal SERS detection tool based on a concept of 'traps and cages' that actively captures and traps analytes close to the SERS substrates [102].

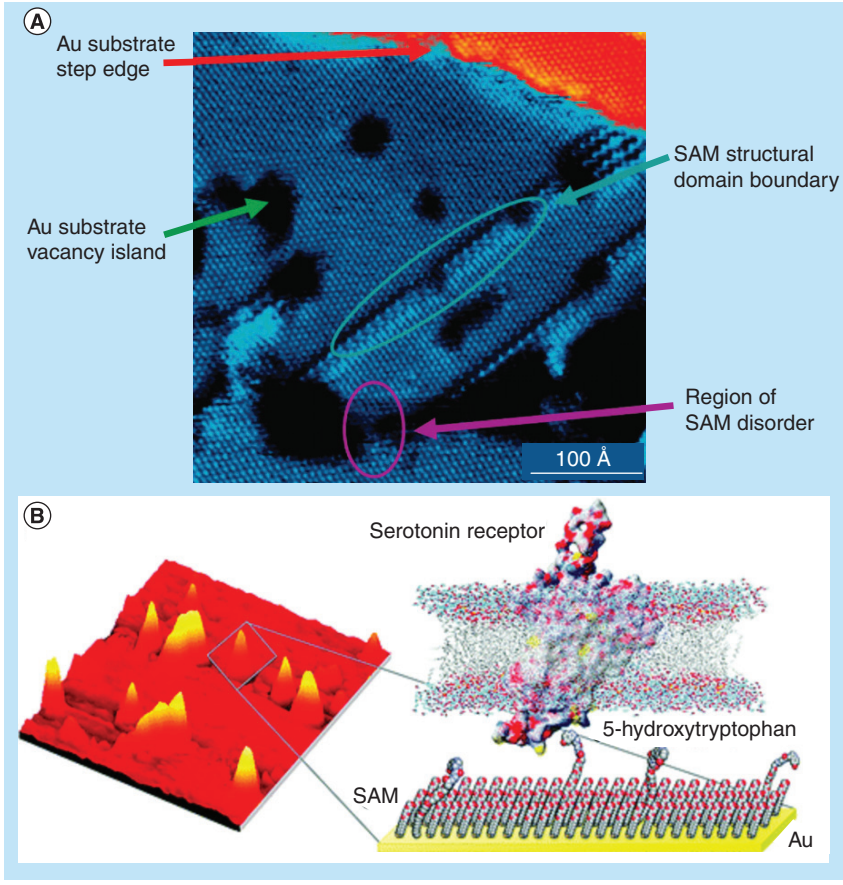

Figure 5. Self-assembled monolayers as versatile interfaces for metals and biomolecules. (A) A molecularly resolved scanning tunneling micrograph of a decanethiol self-assembled monolayer on a Au surface, indicating different types of defects. **(B)** Capturing receptor proteins via surface-tethered small probes. A substrate is functionally modified with serotonin attached to oligo(ethylene glycol)-terminated alkanethiols self-assembled on a Au surface, where serotonin receptor proteins recognize the substrate, demonstrating bioavailability.
SAM: Self-assembled monolayer.
(A) Reproduced with permission from [58] © 2008 American Chemical Society.
(B) Reproduced with permission from [61] © 2010 American Chemical Society.

Besides identifying molecular chemical structures, SERS is capable of differentiating certain conformation-dependent vibration modes in molecules, thus revealing conformational changes [103]. Monitoring the spatiotemporal conformational changes in biomolecules plays a significant role in understanding a variety of coordinate biological processes [68]. Recently, Zheng *et al.* successfully applied SERS to study the reversible photoswitching of isolated azobenzene-functionalized molecules inserted in self-assembled monolayers (FIGURE 10) [104]. By comparing calculated and experimental data, SERS can provide quantitative information on the reversible photoswitching of azobenzene. This study paves the way for detecting transformational and structural changes in functional proteins and other biomolecules. Moreover, it is possible to obtain dynamic information if

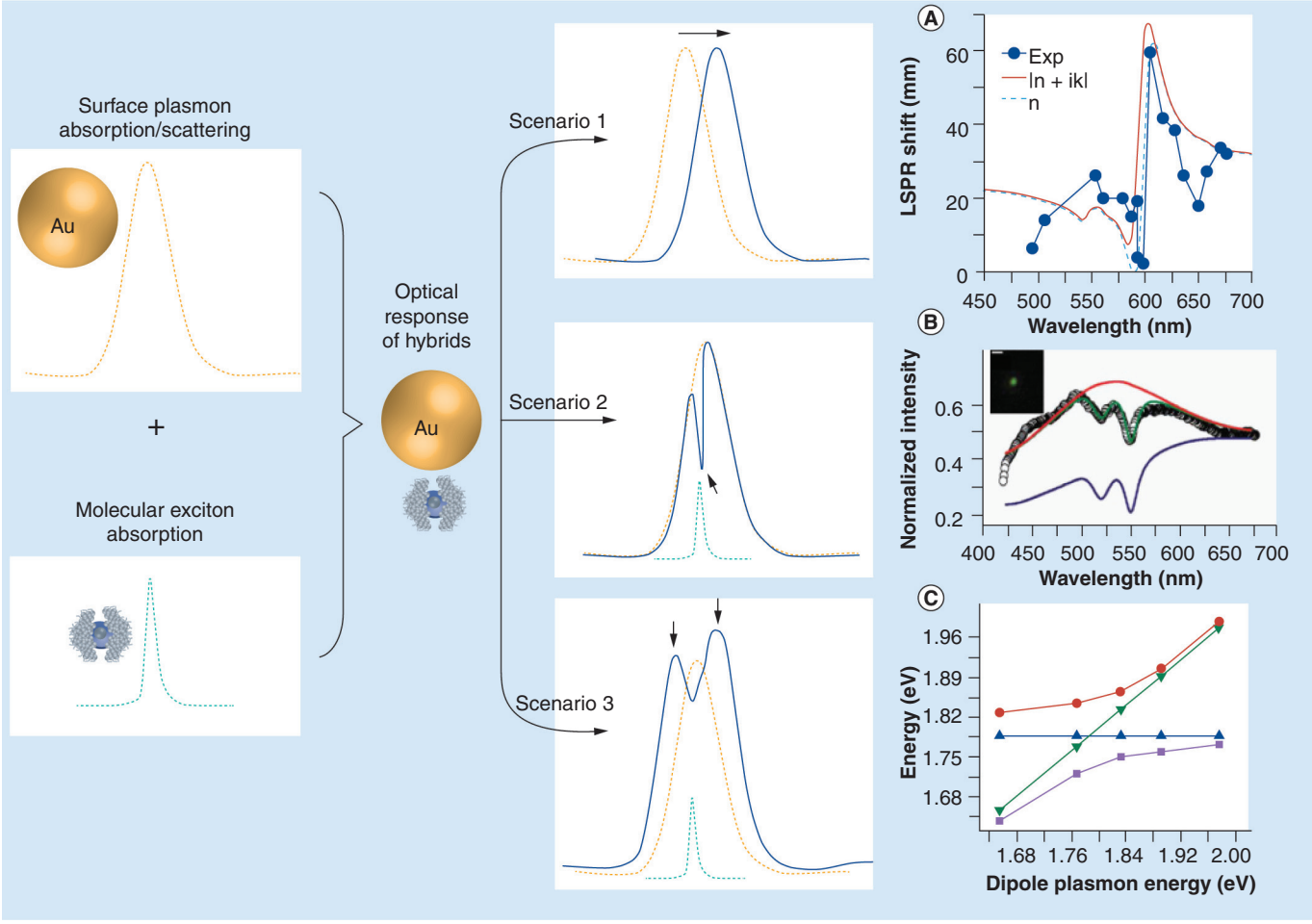

Figure 6. Three types of molecule–plasmon resonance couplings in molecule–metal nanoparticle hybrids. The couplings are reflected in the different localized surface plasmon resonance modulations such as the shift of localized surface plasmon resonance peak wavelength or change of band shape as illustrated in the schematic column. The arrows in the schematic column indicate the large peak shift (scenario 1), the formation of a quenching dip (scenario 2) and the formation of two new peaks (scenario 3). **(A)** The plots of LSPR shift (nm) versus spectral position of the Ag nanoparticles. The solid black line with filled dots is an experimental plot; the other two curves are theoretical plots using two semiempirical models with a scaled refractive index from a Kramers–Kronig analysis. **(B)** The plasmon resonance energy transfer spectra for a 20-nm gold nanoparticle conjugated with reduced cytochrome c molecules. Open circles represent raw data; green solid lines, fitting curve; red solid lines, Lorentzian scattering curve of bare Au nanoparticles; blue solid line, processed absorption spectra for the reduced conjugated cytochrome c by subtracting red curve from the green curve. Inset: scattering image; scale bar: 2 μm. **(C)** Dispersion curve to determine the coherent coupling energy for the localized plasmon/exciton system. Black and green lines: uncoupled exciton.
LSPR: Localized surface plasmon resonance.
(A) Reproduced with permission from [87] © 2006 American Chemical Society. **(B)** Reproduced with permission from [88] © 2007 Nature Publishing Group. **(C)** Reproduced with permission from [91] © 2008 American Chemical Society.

the SERS system is equipped with ultra-fast optics [105].

In summary, SERS is becoming a common analytical tool for studying molecular structures, dynamics, and various biological processes. The plasmonic near-field enhancement is the major driving force that enhances light absorption and scattering processes related to molecular vibrations. Further advances in plasmonics will enable deeper insight into the mechanisms at work in SERS by engineering the hotspots and separating the multiple factors determining the SERS enhancement [42]. While the SERS spectra can identify molecules, spatial information is limited; this poses a problem when studying certain biological processes and when monitoring therapeutic effects. To overcome this limitation, researchers have been developing plasmonic nanoscopy for imaging molecules using LSPR-induced nanoscale localization and enhancement of light [106].

Plasmonic nanoscopy & imaging

Light has significant advantages for imaging applications, including its remote and noninvasive nature and fast response time. Optical

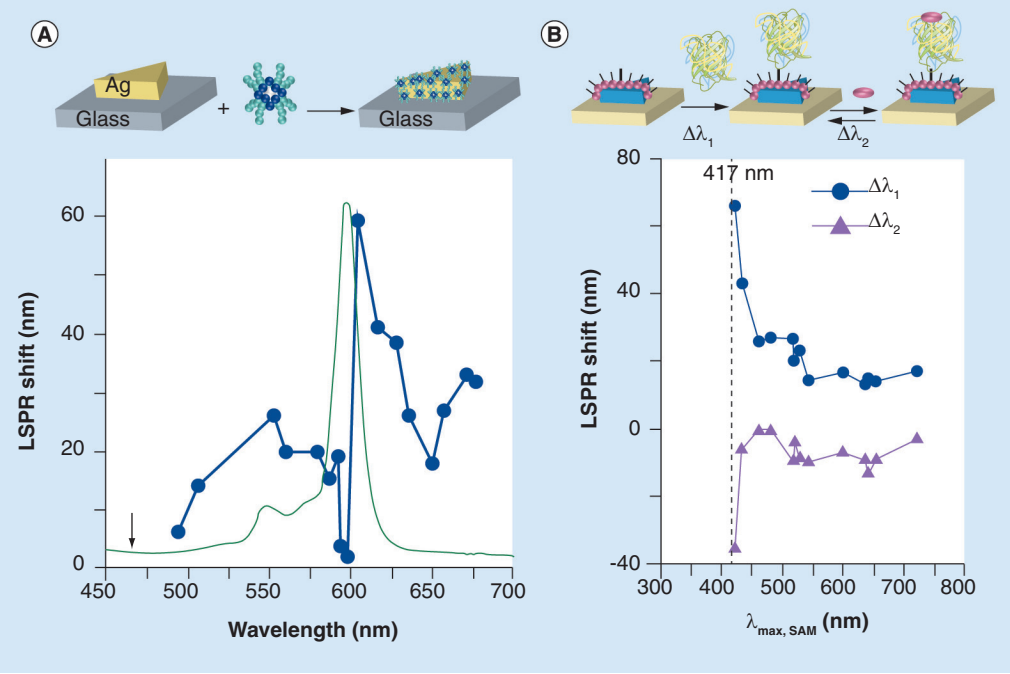

Figure 7. Nanosensors based on localized surface plasmon resonance modulation.
(A) Schematic representation of [2,3,7,8,12,13,17,18-octakis(propyl)porphyrazinato]magnesium (II) (MgPz) adsorbed on silver nanoparticles, and comparison of LSPR shifts induced by a monolayer of MgPz adsorption on the silver nanoparticles with the LSPR of bare silver nanoparticles (dark line with dots). The green line (indicated by black arrow) is the solution absorption spectrum of MgPz.
(B) Schematic representation of cytochrome P450 protein (CYP101) immobilized on a silver biosensor followed by binding camphor, and plots of LSPR shifts against $\lambda_{max,SAM}$ (LSPR of SAM-functionalized nanoparticles), where $\Delta\lambda_1$ is the shift on binding of CYP101 and $\Delta\lambda_2$ is the shift on binding camphor. The vertical dark dotted line denotes the molecular resonance of substrate-free CYP101.
LSPR: Localized surface plasmon resonance; SAM: Self-assembled monolayer.
(A) Reproduced with permission from [87] © 2006 American Chemical Society. **(B)** Reproduced with permission from [85] © 2006 American Chemical Society.

imaging of nanoscale objects, however, exhibits challenges because of the diffraction limitation of light. Advances in nanotechnology have aided in developing techniques that can overcome this limitation to achieve nanoscale optical imaging [107–110]. Under the umbrella of near-field scanning optical microscopy (NSOM), plasmonic nanoscopy is capable of nanoscale biological and medical imaging with high signal-to-noise ratio, high spatial and temporal resolution, and low illumination power [2,111].

Researchers made use of the high resolution inherent to plasmonic nanoscopy to study the fluorescence rate of a single molecule as a function of its distance to a laser-irradiated gold nanoparticle, which also functioned as the nanoscopic probe [112,113]. Near-field fluorescence images were obtained by raster-scanning the sample while maintaining a constant nanoparticle sample separation. By varying the distance between molecule and particle, the researchers demonstrated a continuous transition from fluorescence enhancement to fluorescence quenching. This study helped illuminate some of the physical mechanisms related to the quenching and enhancement of fluorescence from dye molecules by LSPR in nanoparticles [39]. These mechanisms are important in the development of plasmon-enhanced fluorescence tags to take the place of the commonly used isolated fluorescent molecules.

'Chemical vision' is among newer applications of plasmonic nanoscopy, which allows researchers to identify the chemical structure of an object with high spatial resolution [114]. An important development in this subfield has been demonstrated in an example that maps the chemical composition of a silica surface that contains an ultranarrow (30-nm wide) trench of exposed silicon (FIGURE 11) [115]. The plasmonic nanoprobe was mounted on a cantilever that is used both for atomic force microscopy and NSOM/Raman measurements. This allowed the mapping of a silicon surface's chemical fingerprints with roughly 5-nm spatial resolution.

The NSOM-type plasmonic nanoscopes are generally used for *in vitro* analysis of molecules and cells, while suspended metal nanoparticles are

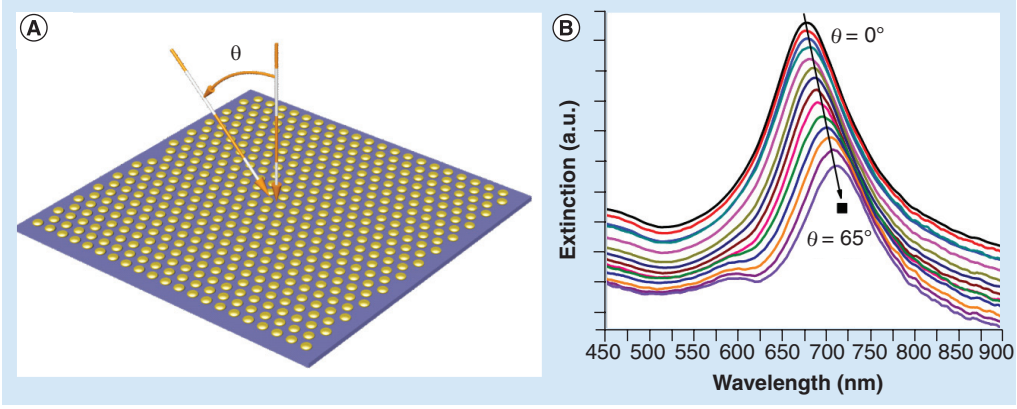

Figure 8. Development of metal nanoparticle arrays with tunable localized surface plasmon resonances as platforms for understanding plasmon–molecule interactions. (A) A schematic of the setup for measuring the angle-resolved extinction spectra of a hexagonally arranged array of Au nanodisks on a glass substrate. The probe light is directed at the array and detected at the zeroth-order transmission while the substrate is rotated out-of-plane with an incident angle θ. **(B)** A series of extinction spectra of the Au nanodisk arrays measured at θ ranging from 0–65° with an interval of 5°.
Reproduced with permission from [95] © 2010 WILEY-VCH Verlag GmbH & Co. KGaA, Weinheim.

usually used as nanoscale probes for *in vivo* imaging. Metal nanoparticles can be made to accumulate selectively in cells or tissues of interest inside the body by functionalizing the particle's surface [116]. Their strong scattering then allows them to provide high-resolution imaging with good photostability, minimum invasiveness and low toxicity. Using this scattering, Estrada and Gratton achieved a high-resolution 3D image of biological fibers such as collagen and actin filaments by moving a single Au nanoparticle along the fibers with near-infrared (NIR) femtosecond pulses and measuring its trajectory [106]. Surgeons may use the imaging capability of metal nanoparticles to help locate tumors and their margins, enabling identification of important adjacent structures and mapping sentinel lymph nodes [69].

In summary, plasmonic nanoscopy is capable of non-invasively imaging molecules with low irradiation power because of plasmon-enhanced molecular absorption, emission and/or scattering of light at the nanoscale. Suspended metal nanoparticles with specific surface functionalizations can serve as probes for 3D *in vivo* molecular imaging. Chemical vision, combining nanoscale imaging and molecular identification, is one of the most important new directions in plasmonic nanoscopy.

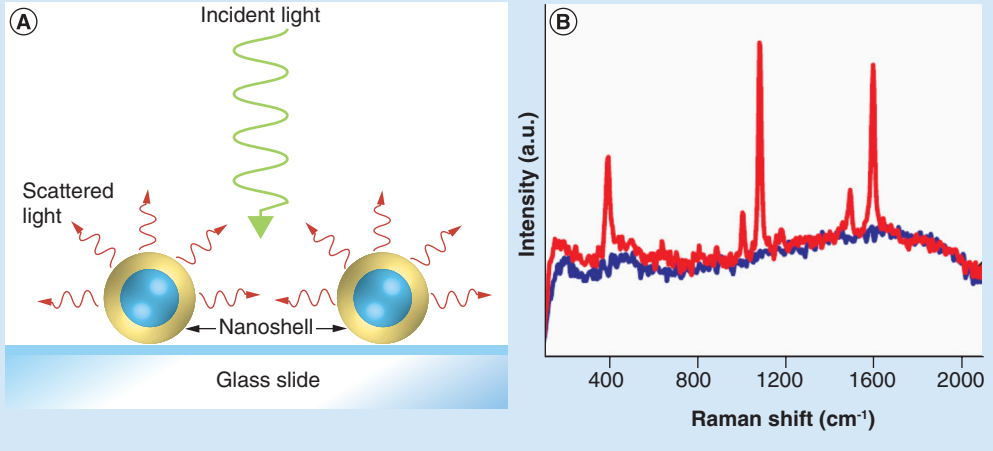

Figure 9. Surface-enhanced Raman spectroscopy. (A) Schematic sample geometry for nanoparticle-based SERS. **(B)** Raman spectrum of *p*-mercaptoaniline collected with no nanoshells (blue) and SERS spectra with nanoshells (red).
a.u.: Absorbance units.
Reproduced with permission from [39] © Nature Publishing Group (2007).

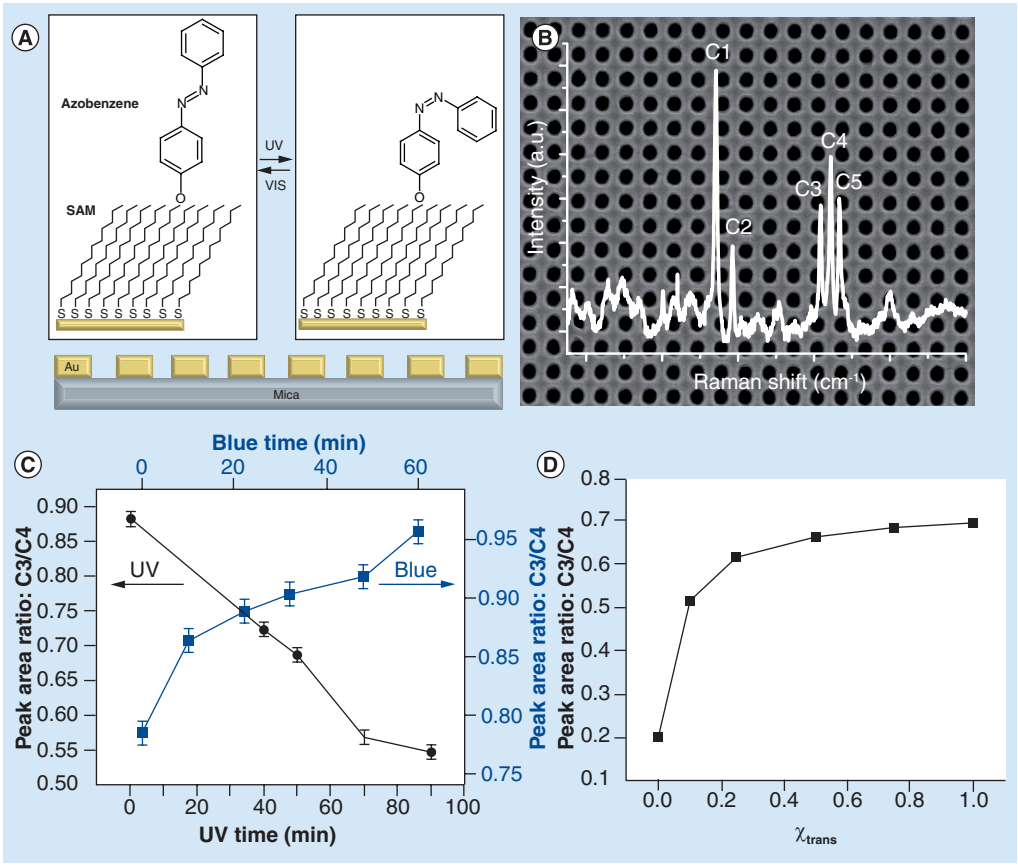

Figure 10. Surface-enhanced Raman spectroscopy for probing photoisomerization of isolated azobenzene. (A) A cross-sectional view of an isolated azobenzene molecule inserted in a SAM of dodecanethiolate on a Au film with a nanohole array. The azobenzene is reversibly photoisomerized between *trans* and *cis* conformations by cycling exposure to UV (365 nm) and blue (450 nm) light. **(B)** A representative scanning electron microscopy image of the nanohole arrays on Au thin films with a Raman spectrum of azobenzenes in a thiolate matrix recorded from the substrate regimens with nanoholes. The five major modes are assigned as C1, C2, C3, C4 and C5. **(C)** The experimental peak area ratio (C3/C4) of the Raman modes C3 and C4 as a function of UV (black circles) and blue (blue squares) light exposure time. **(D)** The simulated (B3LYP/6–31G*) peak area ratio (C3/C4) of the Raman modes C3 and C4 as a function of mole fraction (X_{trans}) of the *trans* isomer.
SAM: Self-assembled monolayer; VIS: Visible.
Reproduced with permission from [104] © 2011 American Chemical Society.

To this point, we have discussed the optical effects of LSPR that enable the development of sensors, spectroscopy and nanoscopy, as well as the current status and future directions of these applications. Coupled with optical near-field effects, metal nanoparticles can rapidly convert absorbed photon energy into heat via multiple photophysical steps: optical absorption and dephasing of LSPR, internal relaxation of the electrons via electron–electron scattering and electron–phonon coupling, and energy dissipation into the environment [117]. Understanding and controlling the effects of the localized thermal energy on molecules and cells near the metal nanoparticles allow us to harness the heat for the development of particle-based photothermal therapy and smart nanocarriers.

Applications based on thermal effects

Photothermal therapeutics

Plasmon-enhanced photothermal effects in metal nanoparticles have already been successfully demonstrated for cancer therapy, where laser excitation is used to kill tumor cells selectively (FIGURE 12A) [30,33]. These metal nanoparticles function like nanoscale lenses, focusing external laser energy at the nanoparticles' LSPR to a small region surrounding the particles. This high EM energy density is converted into thermal energy that heats the metal nanoparticles locally. This process is applied after the particles are in or near the cancer cells, and causes the cells to reach a temperature approximately 15–20°C above physiological temperature, high enough to induce

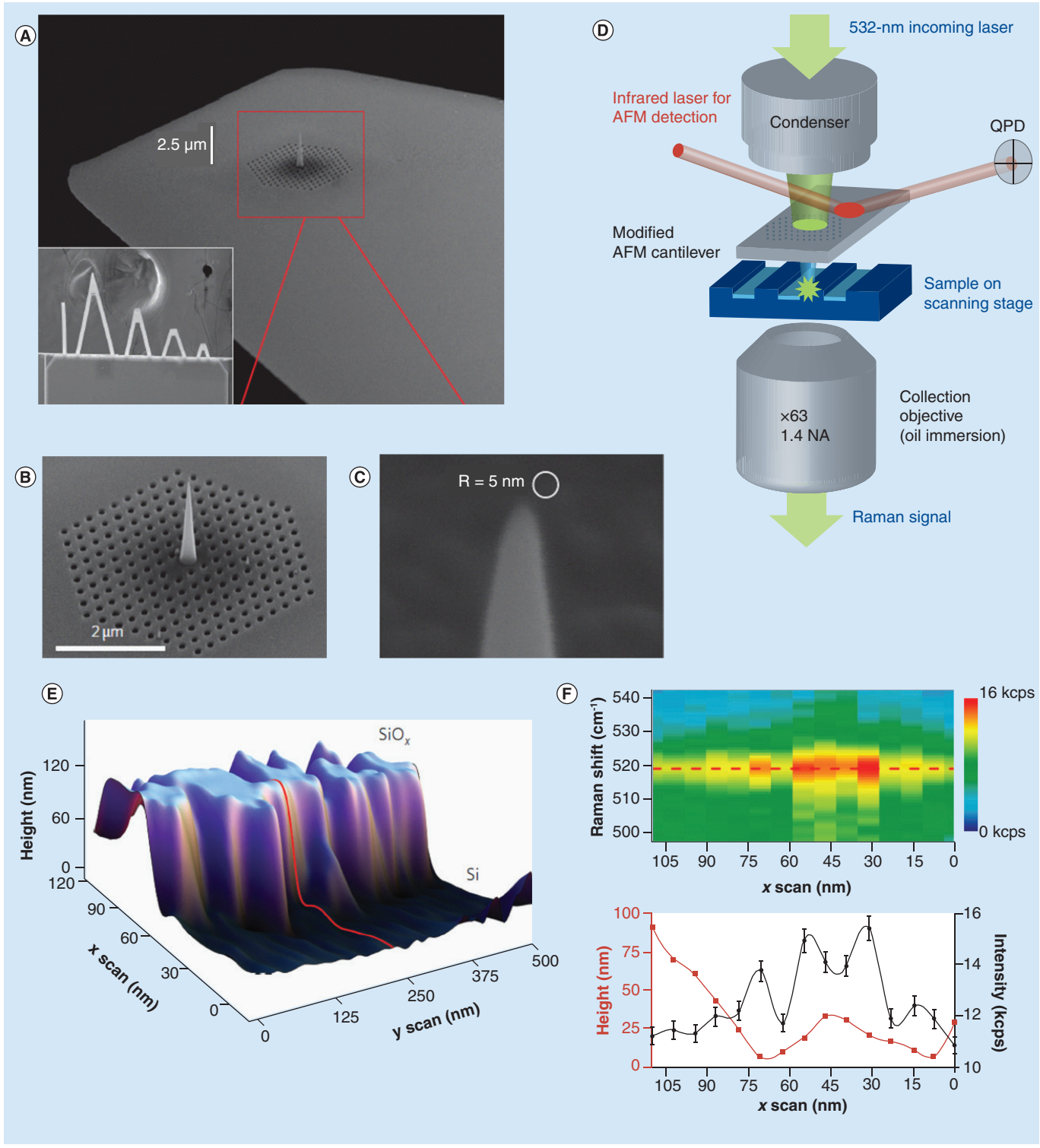

Figure 11. Plasmonic nanoscopy for 'chemical vision'. (A) Scanning electron micrograph of the nanoscope tip. The inset shows multiple tips. **(B,C)** Close-up images of the photonic crystal cavity and the tapered plasmonic waveguide with a conical shape. **(D)** The experimental setup, showing the integration of the photonic–plasmonic device into an AFM–Raman microscope. **(E)** Atomic force micrograph across a submicrometer silicon nanocrystal/SiO_x trench. **(F)** Raman intensity map (top) between 500 and 540 cm^{-1}, as measured simultaneously with AFM topography. The dotted red line corresponds to the red line scan in the topography map of **(E)**. Intensity (bottom) of the c-Si Raman peak at 520 cm^{-1} (black dots) and corresponding AFM line scan (red squares) along the red line of **(E)**.
AFM: Atomic force microscopy; NA: Numerical aperture; QPD: Quadrant photodiode; Si: Silicon; SiO_x: Silicon oxide.
Reproduced with permission from [115] © 2010 Nature Publishing Group.

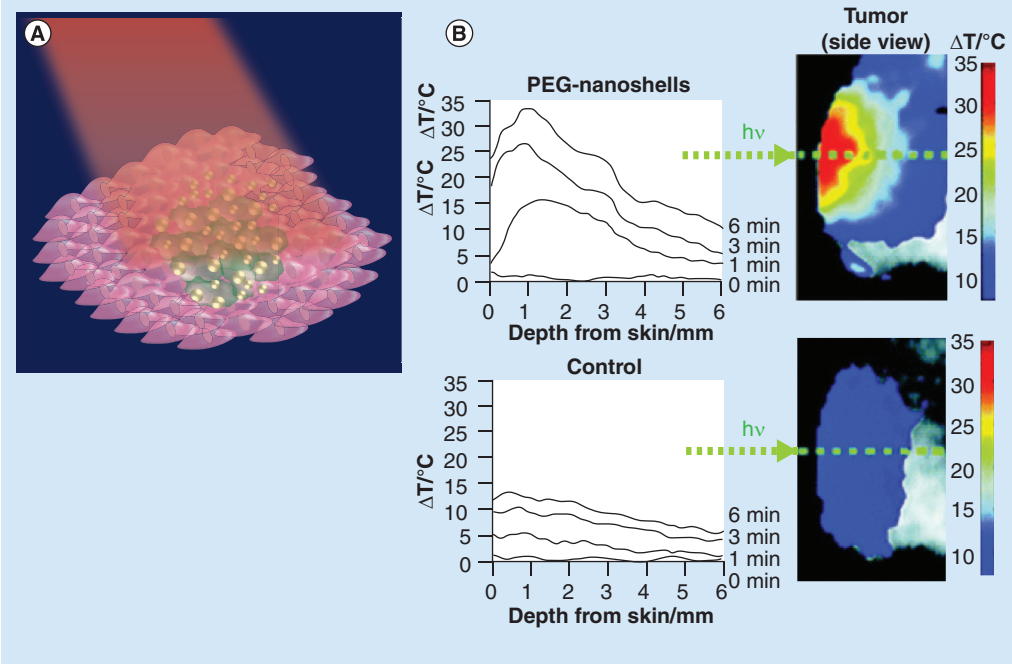

Figure 12. Plasmonic photothermal therapy. (A) Schematic of Au nanoparticles adsorbed selectively on tumors. The localized temperature increase by laser excitation of localized surface plasmon resonance kills the tumor without damaging the healthy cells nearby. **(B)** Real-time, *in vivo* MRI guidance and temperature monitoring of near-infrared laser photothermal cancer therapy using locally administered gold nanoshells.
(A) Reproduced with permission from [124] © 2008 American Chemical Society. **(B)** Reproduced with permission from [27] © 2003 National Academy of Sciences, USA.

apoptosis (FIGURE 12B) [27]. Nanoparticle-assisted photothermal therapy is a drug-free approach that induces cell death by utilizing the localized heat generated upon excitation of LSPR.

Among various metal nanoparticles targeted for photothermal therapy, gold nanoshells, nanorods and nanocages have been the most heavily investigated owing to their widely tunable LSPR, which spans into the NIR range, where absorption in the human body is minimized [14,118–120]. In a critical initial step, Elliot *et al.* quantified the nanoshell–laser interaction to determine the effect of nanoshell concentration and laser power on the photothermal effect [28]. Next, Stern *et al.* evaluated the effect of nanoshell concentration on ablation of a human prostate cancer model in a mouse [29]. El-Sayed and coworkers used anti-EGF receptor antibody-conjugated gold nanoparticles for photothermal therapy of epithelial carcinoma [121]. They found that the malignant cells require less than half the laser energy (continuous visible argon ion laser at 514 nm) to be killed than the benign cells after incubation with the conjugated gold nanoparticles. However, no photothermal destruction was observed for all types of cells in the absence of nanoparticles at the laser energy four-times higher than that required to kill the malignant cells with the anti-EGF receptor/Au conjugates bound [121]. Several excellent review papers on plasmonic photothermal therapy have been published previously [6,116,120,122–124].

To ensure the effectiveness of the photothermal therapy, metal nanoparticles need to accumulate selectively at the tumor site. This is possible through passive accumulation, which occurs due to the leaky tumor vasculature [69]. Malignant tumors rapidly develop new vasculature to supply their expanding mass; these new blood vessels are structurally abnormal and irregularly shaped, characterized by inconsistent diameters and large gaps (up to 2 µm). These gaps are large enough to allow large molecules and nanoparticles from the blood stream to be taken into the tumor. This property is referred to as the enhanced permeability and retention effect, and leads to preferential accumulation of metal nanoparticles in tumors, although accumulation does occur in other normal organs [125]. However, without an appropriate surface coating, nanoparticles in the blood stream are rapidly removed from circulation by the mononuclear phagocyte system, rarely making it to the tumor site [126]. To protect the nanoparticles from this fate, their surfaces can be functionalized with molecules and biomolecules. For instance, nanoparticle delivery may be directed

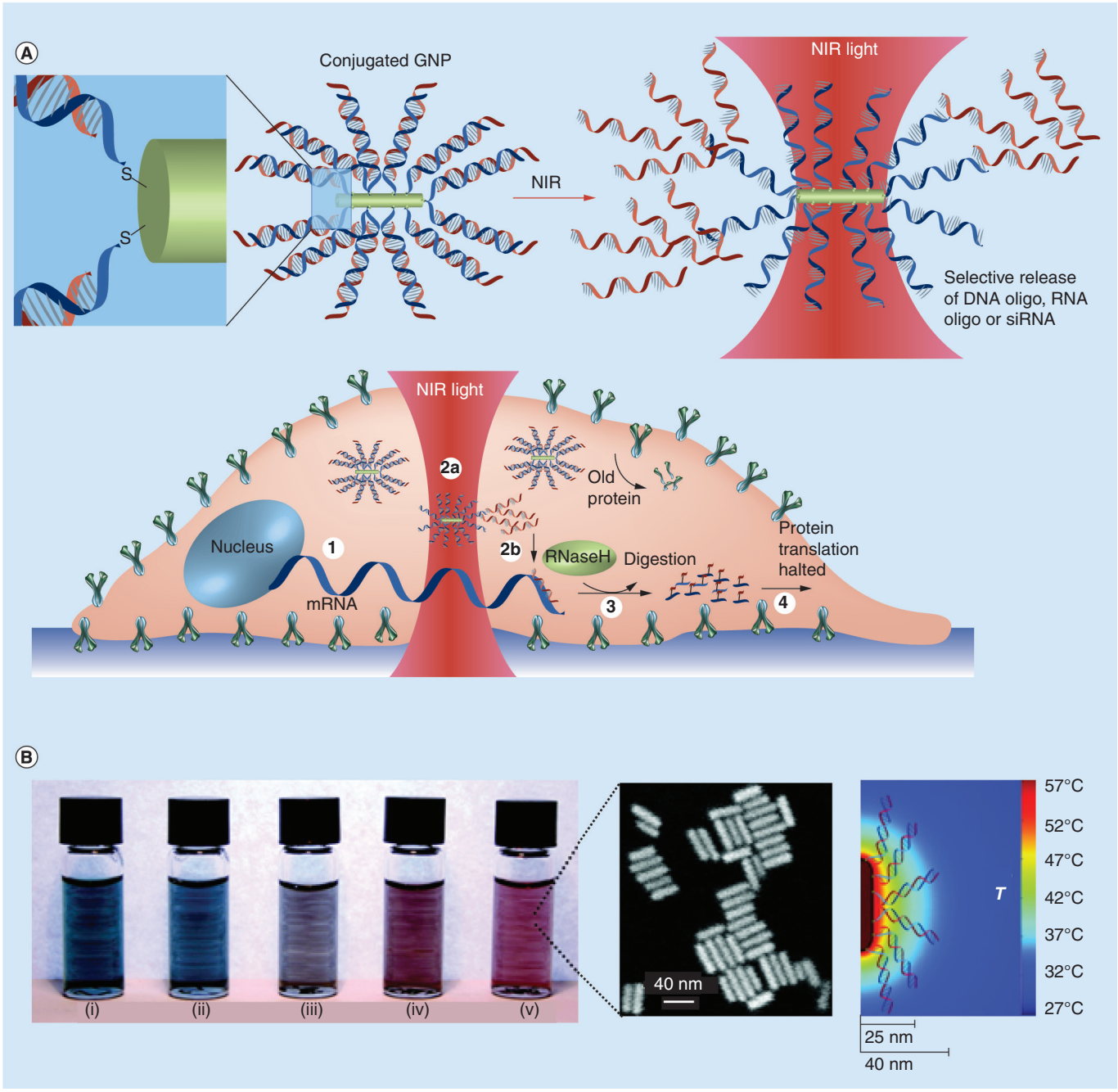

Figure 13. Plasmonic gene therapy. (A) Concept of gene release by oligonucleotides on plasmonic carriers with optical switch activation. **(B)** Left: tunable metal nanorod carriers based on different aspect ratios. Middle: scanning electron microscopy image of nanorod with an aspect ratio (length/diameter) of 3.5. Right: axisymmetric FEMLAB simulation demonstrating localized heat distribution at the nanorod surface at steady state.
GNP: Gold nanoparticle; NIR: Near-infrared.
Reproduced with permission from [135]. © 2009 American Chemical Society.

by conjugating the nanoparticles to antibodies, proteins or ligands specific to surface markers overexpressed by cancer cells [116].

In summary, the localized heat converted from concentrated light at metal nanoparticle surfaces can lead to hyperthermia of nearby cells. Aided by surface functionalization, the particles can target tumors specifically, enabling the eradication of tumor cells without collateral damage to the surrounding healthy cells. For therapies that require chemical drugs or genes rather than the direct thermal treatment, plasmon-enhanced photothermal effects can also be utilized to develop smarter nanocarriers that enable optically-controllable delivery of drug molecules/oligonucleotides.

Smart nanocarriers

Among the many advanced nanotechnology-based approaches towards smart nanocarriers [127–131], metal nanoparticles that use plasmon-enhanced photothermal effects to release drug molecules that were conjugated to their surfaces have shown great promise. Huang and coworkers, for example, devised an aptamer/hairpin DNA–gold nanoparticle conjugate as a smart nanocarrier for the targeted delivery of drugs. When illuminated with light at their LSPR wavelength, the LSPR-induced local heating drastically reduced the nanoparticle–molecule bond stability and the loaded anticancer drug was released; this led to enhanced anti-tumor efficacy with high spatiotemporal resolution and few side effects [132]. Newer developments in this field have led to a drug delivery system that allows multiple drugs to be released in a controlled fashion [17]. In binding drugs to nanoparticles of different shapes, researchers have utilized the fact that metal nanoparticles of different shapes support LSPR at different wavelengths to release specific drugs selectively by illuminating them with monochromatic light. This type of system could be used to provide better temporal control of drug release when battling diseases commonly treated with multiple drugs.

In a similar fashion, metal nanoparticles exhibiting photothermal effects can also function as plasmonic gene switches, regulating intracellular gene activity both temporally and spatially (**Figure 13**) [15,16,133,134]. Because of their large surface-to-volume ratios, nanoparticles are ideal carriers of oligonucleotides such as ssDNA, siRNA and plasmid DNA. For example, short ssDNA (antisense DNA) can be hybridized to thiolated complementary sense DNA and bound to the gold nanoparticle's surface through a gold–thiol covalent bond [135]. While attached to their carriers, oligonucleotides are rendered inactive due to steric hindrance in the tightly packed layer. In the presence of continuous-wave incident light at the LSPR wavelength, antisense DNA is photothermally dehybridized from its carrier and is able to interact freely with the local environment. Thus, remote-controlled NIR light acts as a trigger to release free oligonucleotides and to 'activate' their functionality; this technique enables researchers to silence endogenous intracellular genes on demand. The strategy of photothermal dehybridization offers several notable advantages for gene switches: it requires no chemical modification or reattachment of antisense DNA strands, it does not interfere with nucleic acid functionality and/or gene-silencing efficacy, and it has low cytotoxicity [133].

In summary, plasmon-enhanced photothermal effects enable precise temporal delivery of drugs or gene agents through heat-induced morphology changes in the metal nanoparticles or dehybridization of biomolecules. Advances in plasmonic design, nanofabrication and surface functionalization are enabling the development of smarter nanocarriers through multiplexed wavelength control and complex temporal control of drug delivery; these techniques allow the carriers to deliver multiple drugs with high temporal fidelity to combat a variety of diseases. Future developments will move towards optimizing the nanocarriers for NIR excitation for *in vivo* applications. The relationship of the local temperature distribution to light polarization and intensity for metal nanoparticles of various shapes and sizes should be further studied to enhance applications in specific tumor or gene therapy. In addition to thermal effects, the concentrated EM fields around metal nanoparticles also lead to enhanced optical gradient forces experienced by molecules within the fields. The enhanced near-field optical gradient, and applications of the optical gradient force, such as plasmonic tweezers, will be discussed in the next section.

Applications based on mechanical effects

Plasmonic tweezers

The ability to capture, trap stably and manipulate molecules/biomolecules with nanoscale precision is highly significant for the analysis and understanding of biochemistry and biomechanics. Some examples include the behavior of molecular motors and the mechanical unfolding of globular proteins [35,136]. Among a variety of techniques (e.g., hydrodynamic, electrostatic, electrophoresis and acoustic) that are available for manipulating objects [137,138], optical tweezers have become one of the primary tools for biophysists and have revolutionized the relatively new field of single-molecule biophysics [35,139,140]. For example, Bustamante and coworkers applied optical tweezers with controlled rotation to test the linearity of DNA's twist elasticity; they also measured the torsional modulus and characterized the torque-induced structural transitions, establishing a framework for assays of torque and twist generation by DNA-dependent enzymes [141]. Block and Guydosh determined the binding states of kinesin heads to microtubules with optical tweezers that applied alternating hindering and assisting loads [142].

Optical tweezers generally utilize a tightly focused laser beam to transfer photon momentum to a microparticle/nanoparticle, which experiences two optical forces: a scattering force and a gradient force. These forces work together to trap the particle within the focus spot of the laser beam. Generally, the particle remains trapped in the laser focus, even when the focus is translated, due to the high trap strength. This enables researchers to control the particle's location precisely. However, optical tweezers that trap objects near the focus of a laser beam have several drawbacks, including a trapping volume that is diffraction-limited, inefficiency in trapping objects of reduced size and significant Brownian motion of trapped objects. To trap small molecules and biomolecules, the trap size must be reduced; this requires further focusing of the trapping laser light and increasing of the local laser intensity [143]. Metal nanoparticles demonstrate nanoantenna effects that concentrate light into extremely small areas, providing a promising route for trapping and manipulating biomolecules at reduced laser intensities [34].

Miao *et al.* have demonstrated that the LSPR-enhanced scattering force from a self-assembled gold nanoparticle array can be used to sustain trapping of single micron-sized particles at low laser intensities [144]. To achieve better control of the EM fields for enhanced performance of the plasmonic tweezers, the strong coupling between adjacent plasmonic nanostructures can be exploited. For example, in closely positioned nanoparticle dimers, capacitive effects between the nanoparticles lead to an extremely confined and intense light spot in the gap region, an ideal location for stable trapping of small particles and molecules. Grigorenko *et al.* reported trapping with coupled pairs of gold nanodots in a standard optical tweezers setup [145]. Figure 14A & B show the optical trapping of 200-nm beads near the substrate without and with nanodot pairs, respectively. Brownian motion of a 200-nm bead outside the patterned area is shown in Figure 14A. The plot illustrates the position of a bead trapped at a = 0.7 µm above the glass, measured at different times for a fixed location of the optical trap with a full bandwidth of 10 kHz (green circles).

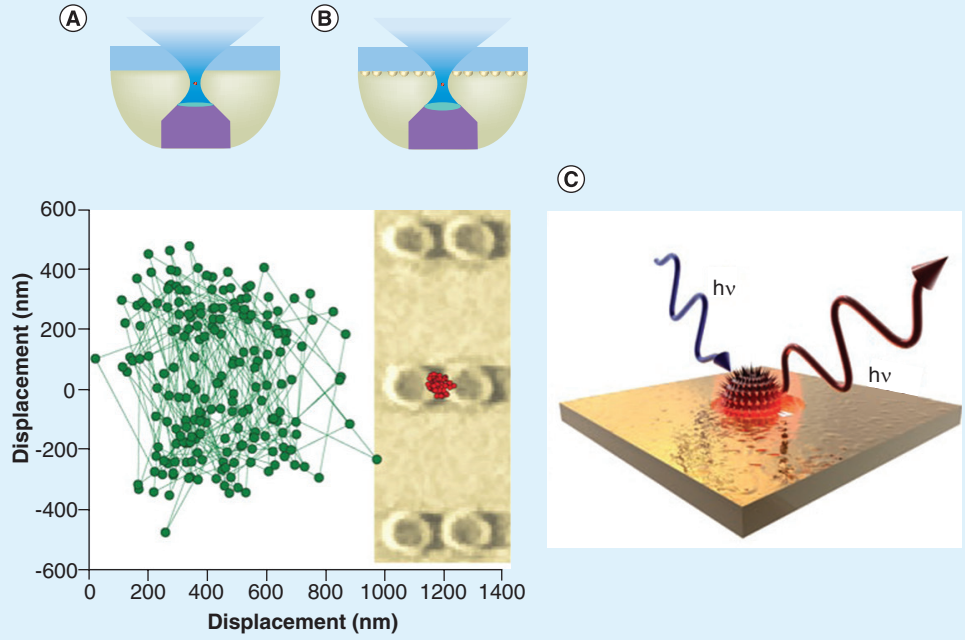

Figure 14. Plasmonic tweezers. (A & B) The optical trapping of 200-nm beads near the substrate without and with nanodot pairs, respectively. Bead position as a function of time at a fixed position, a = 0.7 µm of the beam focus **(A)** above glass (green circles) and **(B)** above a nanodot pair (red circles). Top insets show relevant geometries of the experiment. Scanning electron micrograph of the substrate is scaled to demonstrate the amplitude of the Brownian motion with respect to the size of nanodot pair. **(C)** Schematic illustration of the self-induced back-action-based optical trapping of nanoscale living biological specimens such as viruses.
(A & B) Reproduced with permission from [145] © 2008 Nature Publishing Group. **(C)** Reproduced with permission from [34] © 2011 Nature Publishing Group.

The half-width of the Gaussian displacement distribution for a 200-nm bead was 176 nm. However, when the laser beam was set above the nanodot pair fabricated on the substrate, the half-width reduced to 18 nm under exactly the same conditions (the red circles of FIGURE 14B). Therefore, the optical near-field associated with the nanodot pair reduced the trapping volume beyond the diffraction limit and quenched Brownian motion of the trapped nanoparticles by almost an order of magnitude compared with conventional optical tweezers.

Self-induced back-action (SIBA) in a nanoaperture in a metallic film provides another interesting concept that can be applied towards nanometric optical trapping with reduced heat damage to the trapped specimen [146]. Demonstrated by Quidant and coworkers, SIBA dynamically reconfigures the near-field optical intensity by using the sensitivity of the aperture transmission to its dielectric environment [146]. The presence of an object within the aperture, where the plasmon mode is confined, modifies the effective refractive index, resulting in a red-shift in the transmission peak. As a result, a red-detuned laser makes the local field enhancement stronger when the object is trapped in the aperture, and essentially generates a potential well around the trapped object [147]. This allows the incident laser intensity to be reduced to values associated with a potential depth on the order of the thermal energy. Given its low intensity requirements, SIBA optical trapping should enable trapping of living nanoscale biological specimens, such as viruses, to perform on-chip optical diagnostics (FIGURE 14C).

In summary, plasmonic tweezers are essentially a nanoscale version of optical tweezers. The plasmonically enhanced gradient and scattering forces allow plasmonic tweezers to operate at low power with reduced optical inference or damage to biomolecules and cells. In addition, the 2D nature of surface plasmons facilitates their integration with microfluidics and other biomedical platforms for chip-level applications [20]. Advances in this field have demonstrated both parallel and single trapping of nanoscale objects based on various metal nanostructures (i.e., single nanoparticles, nanoparticle pairs and nanoholes). Future research efforts will be directed towards single-molecule trapping and simultaneous detection or visualization of trapped molecules.

Conclusion & future perspective

Molecular plasmonics that probe the interactions of molecules and surface plasmons of metal nanostructures presents tremendous opportunities for sensing, imaging, manipulating, delivering and smoldering biological molecules, and provides a range of powerful tools for biological and medical studies. We have described and structured the broad range of applications based on three types of molecule–plasmon interactions: optical, thermal and mechanical. Based on the LSPR-induced nanoscale confinement and enhancement of EM fields, metal nanoparticles can transduce biological events, enhance Raman scattering and probe at the single-molecule level. Plasmon-enhanced thermal effects underpin the development of both direct photothermal therapeutic strategies and light-activated drug delivery/gene switches, which have the capability to provide revolutionary tools in the many battles against human disease. Plasmonic tweezers based on LSPR-enhanced optical forces overcome the limitations of conventional optical tweezers, such as the diffraction limit and Brownian motion, enabling low-energy stable trapping of biomolecules for quantitative biology.

As an emerging field situated between molecular nanotechnology and plasmonics, molecular plasmonics has been making extraordinary progress due to advances in metal nanostructure design, fabrication and modeling, in addition to developments in metal nanostructure–molecule complexes, molecular self-assembly and surface functionalization. Examples include: the rational design of metal nanostructures with extremely high sensitivity to molecular adsorption and conformation changes for sensing applications; SERS enhancements due to engineering analyte trapping near EM hotspots; surface functionalization of metal nanoparticles that enhance drug loading, targeting and biocompatibility for *in vivo* imaging and therapy; and precise near-field profile control for multidimensional manipulation of molecules, such as concentration, trapping and rotation.

While new standalone devices will surely emerge because of the continuous advances in molecular plasmonics, future trends will likely move towards highly integrated lab-on-a-chip systems for low-cost and high-efficiency diagnoses and therapies with intrinsic efficacy monitoring, feedback and optimization. Such a system will benefit from the multifunctionalities of LSPR-based phenomena, and can potentially integrate sensing, spectral analysis, molecular manipulation, drug delivery, gene switches and photothermal therapy onto the same nanoparticle platform. This will require strong collaboration between experts in many different fields such as physics,

engineering, chemistry, biology and pharmacology. Initial developments in this direction include theranostic nanomedicine, which encompasses nanoparticles that contain both therapeutic and diagnostic components. These particles serve as optical tracers and imaging contrast agents with their enhanced light scattering and absorption, photothermal vessels for local heating of cancer cells, and drugs/gene carriers with the ability to deliver the agents in a precise temporal manner.

There are a few key areas that need to be evaluated, however, before molecular plasmonic tools and devices advance into commercial domains: nanoparticle biocompatibility and toxicity, effective dosages for theraputics, particle sizes and surface functionalization for efficient targeting, and unintentional particle accumulation and side effects *in vivo*. Appropriately addressing each of these aspects will enable molecular plasmonics to transit from the laboratory domain to clinical applications. With the initial successes and continuous efforts from researchers in multiple disciplines, we are confident that the future of molecular plasmonics in biology and nanomedicine will grow brighter.

Financial & competing interests disclosure

The authors thank the Penn State Center for Nanoscale Science (MRSEC), NIH Director's New Innovator Award (1DP2OD007209-01), the Department of Energy (Grant Nos. DE-SC00-05161 and DE-FG02-07ER15877), the Air Force Office of Scientific Research (FA9550-08-1-0349), the National Science Foundation (ECCS-0801922, ECCS-0609128 and ECCS-0609128), and the Kavli Foundation for support of the work described herein. This material is also based upon work supported by the National Science Foundation Graduate Research Fellowship under Grant No. DGE-0750756. ***The authors have no other relevant affiliations or financial involvement with any organization or entity with a financial interest in or financial conflict with the subject matter or materials discussed in the manuscript apart from those disclosed.***

No writing assistance was utilized in the production of this manuscript.

Executive summary

Background

- Optical excitation of localized surface plasmon resonance (LSPR), the light-coupled oscillation of free electrons confined within metal nanoparticles, results in nanoscale localization and enhancement of electromagnetic fields associated with localized thermal energy and large electromagnetic forces. Molecular plasmonics concerns understanding and control of interactions between molecules and these plasmonic effects.
- We have summarized and structured three types of molecule–plasmon interactions (i.e., optical, mechanical and thermal), which have been harnessed for developing tools used in biology and nanomedicine.

Applications based on optical effects

- Nanosensors based on LSPR modulation have made significant progress due to the development of plasmonic structures with high sensitivity and understanding different molecule–plasmon interaction scenarios.
- Surface-enhanced Raman spectroscopy benefits from the plasmon-induced enhancement of Raman signals from molecules near metal nanoparticles that can focus excitation light onto the molecules. It is a highly sensitive analytical tool with the unique ability of identifying molecular structures.
- Plasmonic nanoscopy uses plasmonic effects at nanoscale tips to shrink light into a nanoscale probe for imaging biomaterials at high resolution.

Applications based on thermal effects

- Photothermal therapy uses localized heat from metal nanoparticles associated with LSPR to induce apoptosis in tumor cells; thus, it is regarded as a drug-free process with minimized side effects.
- Smart nanocarriers are developed by harnessing the thermal energy from LSPR to trigger desorption of drug molecules or dehybridization of biomolecules. They are making progress towards multiplexed, light-controlled drug release.

Applications based on mechanical effects

- Plasmonic tweezers, based on plasmon-enhanced optical forces, trap objects at low power with nanoscale spatial precision, and researchers are working towards manipulation of molecules.

References

Papers of special note have been highlighted as:
- ▪ of interest
- ▪▪ of considerable interest

1 Kreibig U, Vollmer M. *Optical Properties of Metal Clusters.* Springer-Verlag, Berlin Heidelberg, Germany (1995).

2 Stockman MI. Nanoplasmonics: the physics behind the applications. *Phys. Today* 64(2), 39–44 (2011).

▪▪ **Review of the physics behind the applications of plasmonics.**

3 Stiles PL, Dieringer JA, Shah NC, Van Duyne RP. Surface-enhanced Raman spectroscopy. *Annu. Rev. Anal. Chem.* 1, 601–626 (2008).

4 Seol Y, Carpenter AE, Perkins TT. Gold nanoparticles: enhanced optical trapping and sensitivity coupled with significant heating. *Opt. Lett.* 31(16), 2429–2431 (2006).

5 Murray WA, Barnes WL. Plasmonic materials. *Adv. Mater.* 19(22), 3771–3782 (2007).

6 Schwartzberg AM, Zhang JZ. Novel optical properties and emerging applications of metal nanostructures. *J. Phys. Chem. C.* 112(28), 10323–10337 (2008).

7 Kelly KL, Coronado E, Zhao LL, Schatz GC. The optical properties of metal nanoparticles: the influence of size, shape, and dielectric environment. *J. Phys. Chem. B.* 107(3), 668–677 (2003).

8 Jain PK, Huang X, El-Sayed IH, El-Sayad MA. Review of some interesting surface plasmon resonance-enhanced properties of noble metal nanoparticles and their applications to biosystems. *Plasmonics* 2(3), 107–118 (2007).

9 Harry AA. The promise of plasmonics. *Sci. Am.* 296, 56–63 (2007).

10 Maier SA. *Plasmonics: Fundamental and Applications.* Springer Science, NY, USA (2007).

11 Zia R, Schuller JA, Chandran A, Brongersma ML. Plasmonics: the next chip-scale technology. *Mater. Today* 9(7–8), 20–27 (2006).

12 Zayats AV, Smolyaninov II, Maradudin AA. Nano-optics of surface plasmon polaritons. *Phys. Rep. Rev. Sect. Phys. Lett.* 408(3–4), 131–314 (2005).

13 Mayer KM, Hao F, Lee S, Nordlander P, Hafner JH. A single molecule immunoassay by localized surface plasmon resonance. *Nanotechnology* 21(25), 255503 (2010).

14 Becker A, Hessenius C, Licha K *et al.* Receptor-targeted optical imaging of tumors with near-infrared fluorescent ligands. *Nat. Biotechnol.* 19(4), 327–331 (2001).

15 Barhoumi A, Huschka R, Bardhan R, Knight MW, Halas NJ. Light-induced release of DNA from plasmon-resonant nanoparticles: towards light-controlled gene therapy. *Chem. Phys. Lett.* 482(4–6), 171–179 (2009).

16 Huschka R, Zuloaga J, Knight MW, Brown LV, Nordlander P, Halas NJ. Light-induced release of DNA from gold nanoparticles: nanoshells and nanorods. *J. Am. Chem. Soc.* 133(31), 12247–12255 (2011).

17 Wijaya A, Schaffer SB, Pallares IG, Hamad-Schifferli K. Selective release of multiple DNA oligonucleotides from gold nanorods. *ACS Nano* 3(1), 80–86 (2009).

18 Nie S, Emory SR. Probing single molecules and single nanoparticles by surface-enhanced Raman scattering. *Science* 275(5303), 1102–1106 (1997).

19 Law WC, Yong KT, Baev A, Prasad PN. Sensitivity improved surface plasmon resonance biosensor for cancer biomarker detection based on plasmonic enhancement. *ACS Nano* 5(6), 4858–4864 (2011).

20 Wong HMK, Righini M, Gates JC, Smith PGR, Pruneri V, Quidant R. On-a-chip surface plasmon tweezers. *Appl. Phys. Lett.* 99(6), 061107 (2011).

21 Anker JN, Hall WP, Lyandres O, Shah NC, Zhao J, Van Duyne RP. Biosensing with plasmonic nanosensors. *Nat. Mater.* 7(6), 442–453 (2008).

22 Stewart ME, Anderton CR, Thompson LB *et al.* Nanostructured plasmonic sensors. *Chem. Rev.* 108(2), 494–521 (2008).

23 Liao HW, Nehl CL, Hafner JH. Biomedical applications of plasmon resonant metal nanoparticles. *Nanomedicine (Lond).* 1(2), 201–208 (2006).

24 Zhao J, Zhang XY, Yonzon CR, Haes AJ, Van Duyne RP. Localized surface plasmon resonance biosensors. *Nanomedicine (Lond).* 1(2), 219–228 (2006).

25 Mayer KM, Hafner JH. Localized surface plasmon resonance sensors. *Chem. Rev.* 111(6), 3828–3857 (2011).

26 Mayer KM, Lee S, Liao H *et al.* A label-free immunoassay based upon localized surface plasmon resonance of gold nanorods. *ACS Nano* 2(4), 687–692 (2008).

27 Hirsch LR, Stafford RJ, Bankson JA *et al.* Nanoshell-mediated near-infrared thermal therapy of tumors under magnetic resonance guidance. *Proc. Natl Acad. Sci. USA* 100(23), 13549–13554 (2003).

28 Elliott AM, Stafford RJ, Schwartz J *et al.* Laser-induced thermal response and characterization of nanoparticles for cancer treatment using magnetic resonance thermal imaging. *Med. Phys.* 34(7), 3102–3108 (2007).

29 Stern JM, Stanfield J, Kabbani W, Hsieh JT, Cadeddu JA. Selective prostate cancer thermal ablation with laser activated gold nanoshells. *J. Urol.* 179(2), 748–753 (2008).

30 Lowery AR, Gobin AM, Day ES, Shah KY, Halas NJ, West JL. Immunonanoshells for selective photothermal therapy. *Clin. Cancer Res.* 11(24), 9097S–9097S (2005).

31 Khlebtsov B, Zharov V, Melnikov A, Tuchin V, Khlebtsov N. Optical amplification of photothermal therapy with gold nanoparticles and nanoclusters. *Nanotechnology* 17(20), 5167–5179 (2006).

32 Huff TB, Tong L, Zhao Y, Hansen MN, Cheng JX, Wei A. Hyperthermic effects of gold nanorods on tumor cells. *Nanomedicine (Lond).* 2(1), 125–132 (2007).

33 Loo C, Lowery A, Halas N, West J, Drezek R. Immunotargeted nanoshells for integrated cancer imaging and therapy. *Nano Lett.* 5(4), 709–711 (2005).

34 Juan ML, Righini M, Quidant R. Plasmon nano-optical tweezers. *Nat. Photon.* 5(6), 349–356 (2011).

▪ **Excellent description of plasmonic tweezers.**

35 Fazal FM, Block SM. Optical tweezers study life under tension. *Nat. Photon.* 5(6), 318–321 (2011).

36 Alivisatos P. The use of nanocrystals in biological detection. *Nat. Biotechnol.* 22(1), 47–52 (2004).

37 Wang J, Boriskina SV, Wang HY, Reinhard BM. Illuminating epidermal growth factor receptor densities on filopodia through plasmon coupling. *ACS Nano* 5(8), 6619–6628 (2011).

38 Zheng YB, Jensen L, Yan W, Walker TR, Juluri BK, Huang TJ. Chemically tuning the localized surface plasmon resonances of gold nanostructure arrays. *J. Phys. Chem. C* 113(17), 7019–7024 (2009).

39 Lal S, Link S, Halas NJ. Nano-optics from sensing to waveguiding. *Nat. Photon.* 1(11), 641–648 (2007).

40 Cortie MB, Mcdonagh AM. Synthesis and optical properties of hybrid and alloy plasmonic nanoparticles. *Chem. Rev.* 111(6), 3713–3735 (2011).

41 Rycenga M, Cobley CM, Zeng J *et al.* Controlling the synthesis and assembly of silver nanostructures for plasmonic applications. *Chem. Rev.* 111(6), 3669–3712 (2011).

42 Morton SM, Silverstein DW, Jensen L. Theoretical studies of plasmonics using electronic structure methods. *Chem. Rev.* 111(6), 3962–3994 (2011).

▪▪ **Description of electronic structure methods for the studies of plasmonics.**

43 Zheng YB, Huang TJ. Surface plasmons of metal nanostructure arrays: from nanoengineering to active plasmonics. *J. Assoc. Lab. Automat.* 13(4), 215–226 (2008).

44 Zheng YB, Juluri BK, Mao XL, Walker TR, Huang TJ. Systematic investigation of localized surface plasmon resonance of long-range ordered Au nanodisk arrays. *J. Appl. Phys.* 103(1), 014308 (2008).

45 Halas NJ, Lal S, Chang WS, Link S, Nordlander P. Plasmons in strongly coupled metallic nanostructures. *Chem. Rev.* 111(6), 3913–3961 (2011).

46 Halas N. Playing with plasmons. Tuning the optical resonant properties of metallic nanoshells. *MRS Bull.* 30(5), 362–367 (2005).

47 Wiley B, Sun YG, Chen JY *et al.* Shape-controlled synthesis of silver and gold nanostructures. *MRS Bull.* 30(5), 356–361 (2005).

48 Xia YN, Halas NJ. Shape-controlled synthesis and surface plasmonic properties of metallic nanostructures. *MRS Bull.* 30(5), 338–344 (2005).

49 Jones MR, Osberg KD, Macfarlane RJ, Langille MR, Mirkin CA. Templated techniques for the synthesis and assembly of plasmonic nanostructures. *Chem. Rev.* 111(6), 3736–3827 (2011).

50 Hao QZ, Zeng Y, Wang XD *et al.* Characterization of complementary patterned metallic membranes produced simultaneously by a dual fabrication process. *Appl. Phys. Lett.* 97(19), 193101 (2010).

51 Zou SL, Schatz GC. Narrow plasmonic/photonic extinction and scattering line shapes for one and two dimensional silver nanoparticle arrays. *J. Chem. Phys.* 121(24), 12606–12612 (2004).

52 Stockman MI. Spaser action, loss compensation, and stability in plasmonic systems with gain. *Phys. Rev. Lett.* 106(15), 156802 (2011).

53 Bergman DJ, Stockman MI. Surface plasmon amplification by stimulated emission of radiation: quantum generation of coherent surface plasmons in nanosystems. *Phys. Rev. Lett.* 90(2), 027402 (2003).

54 Cygan MT, Dunbar TD, Arnold JJ *et al.* Insertion, conductivity, and structures of conjugated organic oligomers in self-assembled alkanethiol monolayers on $Au^{\{111\}}$. *J. Am. Chem. Soc.* 120(12), 2721–2732 (1998).

55 Donhauser ZJ, Price DW, Tour JM, Weiss PS. Control of alkanethiolate monolayer structure using vapor-phase annealing. *J. Am. Chem. Soc.* 125(38), 11462–11463 (2003).

56 Smith RK, Lewis PA, Weiss PS. Patterning self-assembled monolayers. *Prog. Surf. Sci.* 75(1–2), 1–68 (2004).

57 Love JC, Estroff LA, Kriebel JK, Nuzzo RG, Whitesides GM. Self-assembled monolayers of thiolates on metals as a form of nanotechnology. *Chem. Rev.* 105(4), 1103–1169 (2005).

58 Weiss PS. Functional molecules and assemblies in controlled environments: formation and measurements. *Acc. Chem. Res.* 41(12), 1772–1781 (2008).

▪▪ **Description of self-assemblies and measurements of functional molecules in controlled environments.**

59 Hohman JN, Claridge SA, Kim M, Weiss PS. Cage molecules for self-assembly. *Mat. Sci. Eng. R.* 70(3–6), 188–208 (2010).

60 Saavedra HM, Mullen TJ, Zhang PP, Dewey DC, Claridge SA, Weiss PS. Hybrid strategies in nanolithography. *Rep. Prog. Phys.* 73(3), 036501 (2010).

61 Vaish A, Shuster MJ, Cheunkar S, Singh YS, Weiss PS, Andrews AM. Native serotonin membrane receptors recognize 5-hydroxytryptophan-functionalized substrates: enabling small-molecule recognition. *ACS Chem. Neurosci.* 1(7), 495–504 (2010).

62 Klajn R, Stoddart JF, Grzybowski BA. Nanoparticles functionalised with reversible molecular and supramolecular switches. *Chem. Soc. Rev.* 39(6), 2203–2237 (2010).

63 Sagle LB, Ruvuna LK, Ruemmele JA, Van Duyne RP. Advances in localized surface plasmon resonance spectroscopy biosensing. *Nanomedicine (Lond).* 6(8), 1447–1462 (2011).

64 Willets KA, Van Duyne RP. Localized surface plasmon resonance spectroscopy and sensing. *Annu. Rev. Phys. Chem.* 58, 267–297 (2007).

▪ **Describes the fundamentals of localized surface plasmon resonance and its sensing applications.**

65 Zheng YB, Kiraly B, Cheunkar S, Huang TJ, Weiss PS. Incident-angle-modulated molecular plasmonic switches: a case of weak exciton-plasmon coupling. *Nano Lett.* 11(5), 2061–2065 (2011).

66 Ming T, Zhao L, Xiao M, Wang J. Resonance-coupling-based plasmonic switches. *Small* 6(22), 2514–2519 (2010).

67 Hsiao VKS, Zheng YB, Juluri BK, Huang TJ. Light-driven plasmonic switches based on Au nanodisk arrays and photoresponsive liquid crystals. *Adv. Mater.* 20(18), 3528–3532 (2008).

68 Hall WP, Anker JN, Lin Y, Modica J, Mrksich M, Van Duyne RP. A calcium-modulated plasmonic switch. *J. Am. Chem. Soc.* 130(18), 5836–5837 (2008).

69 Dreaden EC, Mackey MA, Huang XH, Kang B, El-Sayed MA. Beating cancer in multiple ways using nanogold. *Chem. Soc. Rev.* 40(7), 3391–3404 (2011).

▪ **Describes the multiple ways of using nanogold for diagnosis and treatment of cancer.**

70 Yonzon CR, Stuart DA, Zhang XY, Mcfarland AD, Haynes CL, Van Duyne RP. Towards advanced chemical and biological nanosensors – an overview. *Talanta* 67(3), 438–448 (2005).

71 Haes AJ, Chang L, Klein WL, Van Duyne RP. Detection of a biomarker for Alzheimer's disease from synthetic and clinical samples using a nanoscale optical biosensor. *J. Am. Chem. Soc.* 127(7), 2264–2271 (2005).

72 Wittenberg NJ, Im H, Johnson TW *et al.* Facile assembly of micro- and nanoarrays for sensing with natural cell membranes. *ACS Nano* 5(9), 7555–7564 (2011).

73 Yonzon CR, Jeoungf E, Zou SL, Schatz GC, Mrksich M, Van Duyne RP. A comparative analysis of localized and propagating surface plasmon resonance sensors: the binding of concanavalin a to a monosaccharide functionalized self-assembled monolayer. *J. Am. Chem. Soc.* 126(39), 12669–12676 (2004).

74 Sonnichsen C, Reinhard BM, Liphardt J, Alivisatos AP. A molecular ruler based on plasmon coupling of single gold and silver nanoparticles. *Nat. Biotechnol.* 23(6), 741–745 (2005).

75 Reinhard BM, Sheikholeslami S, Mastroianni A, Alivisatos AP, Liphardt J. Use of plasmon coupling to reveal the dynamics of DNA bending and cleavage by single EcoRV restriction enzymes. *Proc. Natl Acad. Sci. USA* 104(8), 2667–2672 (2007).

76 Liu N, Hentschel M, Weiss T, Alivisatos AP, Giessen H. Three-dimensional plasmon rulers. *Science* 332(6036), 1407–1410 (2011).

77 Pryce IM, Kelaita YA, Aydin K, Atwater HA. Compliant metamaterials for resonantly enhanced infrared absorption spectroscopy and refractive index sensing. *ACS Nano* 5(10), 8167–8174 (2011).

78 Hao F, Nehl CL, Hafner JH, Nordlander P. Plasmon resonances of a gold nanostar. *Nano Lett.* 7(3), 729–732 (2007).

79 Bukasov R, Shumaker-Parry JS. Highly tunable infrared extinction properties of gold nanocrescents. *Nano Lett.* 7(5), 1113–1118 (2007).

80 Larsson EM, Alegret J, Kall M, Sutherland DS. Sensing characteristics of NIR localized surface plasmon resonances in gold nanorings for application as ultrasensitive biosensors. *Nano Lett.* 7(5), 1256–1263 (2007).

81 Liu N, Tang ML, Hentschel M, Giessen H, Alivisatos AP. Nanoantenna-enhanced gas sensing in a single tailored nanofocus. *Nat. Mater.* 10(8), 631–636 (2011).

82 Liu N, Weiss T, Mesch M *et al.* Planar metamaterial analogue of electromagnetically induced transparency for plasmonic sensing. *Nano Lett.* 10(4), 1103–1107 (2010).

83 Dondapati SK, Sau TK, Hrelescu C, Klar TA, Stefani FD, Feldmann J. Label-free biosensing based on single gold nanostars as plasmonic transducers. *ACS Nano* 4(11), 6318–6322 (2010).

84 Dahlin AB, Tegenfeldt JO, Hook F. Improving the instrumental resolution of sensors based on localized surface plasmon resonance. *Anal. Chem.* 78(13), 4416–4423 (2006).

85 Zhao J, Das A, Zhang X, Schatz GC, Sligar SG, Van Duyne RP. Resonance surface plasmon spectroscopy: low molecular weight substrate binding to cytochrome P450. *J. Am. Chem. Soc.* 128(34), 11004–11005 (2006).

86 Choi Y, Park Y, Kang T, Lee LP. Selective and sensitive detection of metal ions by plasmonic resonance energy transfer-based nanospectroscopy. *Nat. Nanotechnol.* 4(11), 742–746 (2009).

87 Haes AJ, Zou SL, Zhao J, Schatz GC, Van Duyne RP. Localized surface plasmon resonance spectroscopy near molecular resonances. *J. Am. Chem. Soc.* 128(33), 10905–10914 (2006).

88 Liu GL, Long YT, Choi Y, Kang T, Lee LP. Quantized plasmon quenching dips nanospectroscopy via plasmon resonance energy transfer. *Nat. Methods* 4(12), 1015–1017 (2007).

89 Choi YH, Kang T, Lee LP. Plasmon resonance energy transfer (PRET)-based molecular imaging of cytochrome c in living cells. *Nano Lett.* 9(1), 85–90 (2009).

90 Wiederrecht GP, Wurtz GA, Hranisavljevic J. Coherent coupling of molecular excitons to electronic polarizations of noble metal nanoparticles. *Nano Lett.* 4(11), 2121–2125 (2004).

91 Fofang NT, Park TH, Neumann O, Mirin NA, Nordlander P, Halas NJ. Plexcitonic nanoparticles: plasmon-exciton coupling in nanoshell-J-aggregate complexes. *Nano Lett.* 8(10), 3481–3487 (2008).

92 Ni W, Ambjornsson T, Apell SP, Chen H, Wang J. Observing plasmonic – molecular resonance coupling on single gold nanorods. *Nano Lett.* 10(1), 77–84 (2009).

93 Ni W, Yang Z, Chen H, Li L, Wang J. Coupling between molecular and plasmonic resonances in freestanding dye – gold nanorod hybrid nanostructures. *J. Am. Chem. Soc.* 130(21), 6692–6693 (2008).

94 Ni W, Chen H, Su J, Sun Z, Wang J, Wu H. Effects of dyes, gold nanocrystals, pH, and metal ions on plasmonic and molecular resonance coupling. *J. Am. Chem. Soc.* 132(13), 4806–4814 (2010).

95 Zheng YB, Juluri BK, Jensen LL *et al.* Dynamically tuning plasmon-exciton coupling in arrays of nanodisk-J-aggregate complexes. *Adv. Mater.* 22(32), 3603–3607 (2010).

96 Anker JN, Hall WP, Lambert MP *et al.* Detection and identification of bioanalytes with high resolution LSPR spectroscopy and MALDI mass spectrometry. *J. Phys. Chem. C.* 113(15), 5891–5894 (2009).

97 Gardiner DJ. *Practical Raman Spectroscopy.* Graves PR (Ed.). Springer-Verlag, Berlin, Heidelberg, Germany (1989).

98 Lal S, Grady NK, Kundu J, Levin CS, Lassiter JB, Halas NJ. Tailoring plasmonic substrates for surface enhanced spectroscopies. *Chem. Soc. Rev.* 37(5), 898–911 (2008).

99 Kneipp J, Kneipp H, Kneipp K. SERS – a single-molecule and nanoscale tool for bioanalytics. *Chem. Soc. Rev.* 37(5), 1052–1060 (2008).

100 Jackson JB, Halas NJ. Surface-enhanced Raman scattering on tunable plasmonic nanoparticle substrates. *Proc. Natl Acad. Sci. USA* 101(52), 17930–17935 (2004).

101 Le Ru EC, Grand J, Sow I *et al.* A scheme for detecting every single target molecule with surface-enhanced Raman spectroscopy. *Nano Lett.* 11(11), 5013–5019 (2011).

102 Alvarez-Puebla RA, Liz-Marzan LM. Traps and cages for universal SERS detection. *Chem. Soc. Rev.* 41(1), 43–51 (2012).

103 Tamai N, Miyasaka H. Ultrafast dynamics of photochromic systems. *Chem. Rev.* 100(5), 1875–1890 (2000).

104 Zheng YB, Payton JL, Chung CH *et al.* Surface-enhanced Raman spectroscopy to probe reversibly photoswitchable azobenzene in controlled nanoscale environments. *Nano Lett.* 11(8), 3447–3452 (2011).

105 Katayama I, Koga S, Shudo K *et al.* Ultrafast dynamics of surface-enhanced Raman scattering due to Au nanostructures. *Nano Lett.* 11(7), 2648–2654 (2011).

106 Estrada LC, Gratton E. 3D nanometer images of biological fibers by directed motion of gold nanoparticles. *Nano Lett.* 11(11), 4656–4660 (2011).

107 Liu ZW, Lee H, Xiong Y, Sun C, Zhang X. Far-field optical hyperlens magnifying sub-diffraction-limited objects. *Science* 315(5819), 1686–1686 (2007).

108 Fang N, Lee H, Sun C, Zhang X. Sub-diffraction-limited optical imaging with a silver superlens. *Science* 308(5721), 534–537 (2005).

109 Huang B, Babcock H, Zhuang X. Breaking the diffraction barrier: super-resolution imaging of cells. *Cell* 143(7), 1047–1058 (2010).

110 Huang B, Wang W, Bates M, Zhuang X. Three-dimensional super-resolution imaging by stochastic optical reconstruction microscopy. *Science* 319(5864), 810–813 (2008).

111 Novotny L, Stranick SJ. Near-field optical microscopy and spectroscopy with pointed probes. *Annu. Rev. Phys. Chem.* 57, 303–331 (2006).

112 Anger P, Bharadwaj P, Novotny L. Enhancement and quenching of single-molecule fluorescence. *Phys. Rev. Lett.* 96(11), 113002 (2006).

113 Eghlidi H, Lee KG, Chen XW, Gotzinger S, Sandoghdar V. Resolution and enhancement in nanoantenna-based fluorescence microscopy. *Nano Lett.* 9(12), 4007–4011 (2009).

114 Pettinger B. Tip-enhanced Raman spectroscopy (TERS). *Top. Appl. Phys.*103, 217–240 (2006).

115 De Angelis F, Das G, Candeloro P *et al.* Nanoscale chemical mapping using three-dimensional adiabatic compression of surface plasmon polaritons. *Nat. Nanotechnol.* 5(1), 67–72 (2010).

116 Bardhan R, Lal S, Joshi A, Halas NJ. Theranostic nanoshells: from probe design to imaging and treatment of cancer. *Acc. Chem. Res.* 44(10), 936–946 (2011).

▪▪ **Excellent description of theranostic nanoshells.**

117 Hartland GV. Optical studies of dynamics in noble metal nanostructures. *Chem. Rev.* 111(6), 3858–3887 (2011).

118 Hu M, Chen JY, Li ZY *et al.* Gold nanostructures: engineering their plasmonic properties for biomedical applications. *Chem. Soc. Rev.* 35(11), 1084–1094 (2006).

119 Averitt RD, Westcott SL, Halas NJ. Linear optical properties of gold nanoshells. *J. Opt. Soc. Am. B* 16(10), 1824–1832 (1999).

120 Xia Y, Li W, Cobley CM *et al.* Gold nanocages: from synthesis to theranostic applications. *Acc. Chem. Res.* 44(10), 914–924 (2011).

121 El-Sayed IH, Huang X, El-Sayed MA. Selective laser photo-thermal therapy of epithelial carcinoma using anti-EGFR antibody conjugated gold nanoparticles. *Cancer Lett.* 239(1), 129–135 (2006).

122 Huang XH, Jain PK, El-Sayed IH, El-Sayed MA. Gold nanoparticles: interesting optical properties and recent applications in cancer diagnostic and therapy. *Nanomedicine (Lond).* 2(5), 681–693 (2007).

123 Huang XH, Jain PK, El-Sayed IH, El-Sayed MA. Plasmonic photothermal therapy (PPTT) using gold nanoparticles. *Laser Med. Sci.* 23(3), 217–228 (2008).

124 Lal S, Clare SE, Halas NJ. Nanoshell-enabled photothermal cancer therapy: impending clinical impact. *Acc. Chem. Res.* 41(12), 1842–1851 (2008).

125 Maeda H. The enhanced permeability and retention (EPR) effect in tumor vasculature: the key role of tumor-selective macromolecular drug targeting. *Adv. Enzyme Regul.* 41, 189–207 (2001).

126 Olivier JC. Drug transport to brain with targeted nanoparticles. *NeuroRx* 2(1), 108–119 (2005).

127 Zheng YB, Kiraly B, Huang TJ. Molecular machines drive smart drug delivery. *Nanomedicine (Lond).* 5(9), 1309–1312 (2010).

128 Burakowska E, Zimmerman SC, Haag R. Photoresponsive crosslinked hyperbranched

polyglycerols as smart nanocarriers for guest binding and controlled release. *Small* 5(19), 2199–2204 (2009).

129 Kataoka K, Itaka K, Nishiyama N, Yamasaki Y, Oishi M, Nagasaki Y. Smart polymeric micelles as nanocarriers for oligonucleotides and siRNA delivery. *Nucleic Acids Symp. Ser. (Oxf.)* 49(1), 17–18 (2005).

130 Sawant RM, Hurley JP, Salmaso S *et al.* 'SMART' drug delivery systems: double-targeted pH-responsive pharmaceutical nanocarriers. *Bioconjug. Chem.* 17(4), 943–949 (2006).

131 Leung SJ, Kachur XM, Bobnick MC, Romanowski M. Wavelength-selective light-induced release from plasmon resonant liposomes. *Adv. Funct. Mater.* 21(6), 1113–1121 (2011).

132 Luo YL, Shiao YS, Huang YF. Release of photoactivatable drugs from plasmonic nanoparticles for targeted cancer therapy. *ACS Nano* 5(10), 7796–7804 (2011).

133 Lee SE, Lee LP. Nanoplasmonic gene regulation. *Curr. Opin. Chem. Biol.* 14(5), 623–633 (2010).

134 Jones MR, Millstone JE, Giljohann DA, Seferos DS, Young KL, Mirkin CA. Plasmonically controlled nucleic acid dehybridization with gold nanoprisms. *Chemphyschem* 10(9–10), 1461–1465 (2009).

135 Lee SE, Liu GL, Kim F, Lee LP. Remote optical switch for localized and selective control of gene interference. *Nano Lett.* 9(2), 562–570 (2009).

136 Moffitt JR, Chemla YR, Smith SB, Bustamante C. Recent advances in optical tweezers. *Annu. Rev. Biochem.* 77, 205–228 (2008).

137 Chiou PY, Ohta AT, Wu MC. Massively parallel manipulation of single cells and microparticles using optical images. *Nature* 436(7049), 370–372 (2005).

138 Shi JJ, Ahmed D, Mao X, Lin SCS, Lawit A, Huang TJ. Acoustic tweezers: patterning cells and microparticles using standing surface acoustic waves (SSAW). *Lab Chip* 9(20), 2890–2895 (2009).

139 Won R, Ashkin A. How it all began. *Nat. Photon.* 5(6), 316–317 (2011).

140 Claridge SA, Schwartz JJ, Weiss PS. Electrons, photons, and force: quantitative single-molecule measurements from physics to biology. *ACS Nano* 5(2), 693–729 (2011).

141 Bryant Z, Stone MD, Gore J, Smith SB, Cozzarelli NR, Bustamante C. Structural transitions and elasticity from torque measurements on DNA. *Nature* 424(6946), 338–341 (2003).

142 Guydosh NR, Block SM. Direct observation of the binding state of the kinesin head to the microtubule. *Nature* 461(7260), 125–128 (2009).

143 Novotny L, Bian RX, Xie XS. Theory of nanometric optical tweezers. *Phys. Rev. Lett.* 79(4), 645–648 (1997).

144 Miao XY, Lin LY. Large dielectrophoresis force and torque induced by localized surface plasmon resonance of Au nanoparticle array. *Opt. Lett.* 32(3), 295–297 (2007).

145 Grigorenko AN, Roberts NW, Dickinson MR, Zhang Y. Nanometric optical tweezers based on nanostructured substrates. *Nat. Photon.* 2(6), 365–370 (2008).

146 Juan ML, Gordon R, Pang YJ, Eftekhari F, Quidant R. Self-induced back-action optical trapping of dielectric nanoparticles. *Nat. Phys.* 5(12), 915–919 (2009).

147 De Abajo FJGI. Light transmission through a single cylindrical hole in a metallic film. *Opt. Express* 10(25), 1475–1484 (2002).